MARTIN MARIETTA ENERGY SYSTEMS LIBRARIES
3 4456 0361476 5

4

CENTRAL RESEARCH LIBRARY
DOCUMENT COLLECTION

ORNL-2919
UC-37 - Instruments

THE ANGULAR DISTRIBUTION OF ALPHA PARTICLES EMITTED BY ORIENTED Np^{237} NUCLEI

S. H. Hanauer
J. W. T. Dabbs
L. D. Roberts
G. W. Parker

CENTRAL RESEARCH LIBRARY
DOCUMENT COLLECTION
LIBRARY LOAN COPY
DO NOT TRANSFER TO ANOTHER PERSON
If you wish someone else to see this document, send in name with document and the library will arrange a loan.

OAK RIDGE NATIONAL LABORATORY
operated by
UNION CARBIDE CORPORATION
for the
U.S. ATOMIC ENERGY COMMISSION

Printed in USA. Price $2.25. Available from the

Office of Technical Services
Department of Commerce
Washington 25, D.C.

LEGAL NOTICE

This report was prepared as an account of Government sponsored work. Neither the United States, nor the Commission, nor any person acting on behalf of the Commission:

A. Makes any warranty or representation, expressed or implied, with respect to the accuracy, completeness, or usefulness of the information contained in this report, or that the use of any information, apparatus, method, or process disclosed in this report may not infringe privately owned rights; or

B. Assumes any liabilities with respect to the use of, or for damages resulting from the use of any information, apparatus, method, or process disclosed in this report.

As used in the above, "person acting on behalf of the Commission" includes any employee or contractor of the Commission, or employee of such contractor, to the extent that such employee or contractor of the Commission, or employee of such contractor prepares, disseminates, or provides access to, any information pursuant to his employment or contract with the Commission, or his employment with such contractor.

ORNL-2919

Contract No. W-7405-eng-26

PHYSICS DIVISION

THE ANGULAR DISTRIBUTION OF ALPHA PARTICLES EMITTED BY ORIENTED Np^{237} NUCLEI

S. H. Hanauer
J. W. T. Dabbs
L. D. Roberts
G. W. Parker

Submitted as a thesis to the Faculty of the Graduate Council of the University of Tennessee in partial fulfillment of the requirements for the degree of Doctor of Philosophy in Physics.

DATE ISSUED
MAY 10 1960

[redacted]

OAK RIDGE NATIONAL LABORATORY
Oak Ridge, Tennessee
operated by
UNION CARBIDE CORPORATION
for the
U.S. ATOMIC ENERGY COMMISSION

MARTIN MARIETTA ENERGY SYSTEMS LIBRARIES
3 4456 0361476 5

ABSTRACT

Neptunium-237 nuclei were aligned when a monocrystalline sample of neptunyl rubidium nitrate was cooled to 0.2 - 4.2°K. The rotatable sample was placed in a capsule filled with helium-3 gas for heat transfer. Also in the capsule were a germanium surface-barrier alpha-particle counter, a thermometer, and rotation indicators. The capsule was in thermal contact with 1/2 mole of manganous ammonium sulphate hexahydrate for cooling by adiabatic demagnetization. At all temperatures in the range studied, the alpha particles were observed to be emitted preferentially perpendicular to the crystalline c axis. Comparison of the temperature variation of the anisotropy with predictions from an experimentally determined spin Hamiltonian made possible an unambiguous assignment, $A < 0$, $P > 0$, of the signs of the hyperfine coupling constants in neptunyl rubidium nitrate. These sign assignments and the experimentally observed preferred direction for alpha-particle emission place current ideas about the electronic structure of uranyl-like ions in conflict with a simple barrier-penetration picture of alpha-particle emission.

ACKNOWLEDGEMENTS

The authors are indebted to Mr. F. J. Walter for making the solid-state alpha-particle counter which was used in this experiment, and for many helpful discussions and much assistance.

The low-noise pre-amplifier was designed and constructed by Mr. E. Fairstein.

The alpha energy analysis of the sample was obtained by Mrs. L. C. Davis. Mr. S. A. Reynolds performed the beta and gamma analysis of the sample.

The authors appreciate the excellent technical assistance provided by Mr. C. R. Hill and Mr. C. T. Hall of the Physics Division Shop.

TABLE OF CONTENTS

CHAPTER		PAGE
I.	INTRODUCTION	1
II.	EMISSION OF ALPHA PARTICLES BY ORIENTED NUCLEI	5
	Nuclear Theory Based on the Barrier Penetration Model	5
	Angular Momentum Theory	6
	Geometry Correction	11
III.	NUCLEAR ALIGNMENT IN NEPTUNYL RUBIDIUM NITRATE	14
IV.	EXPERIMENTAL ARRANGEMENT	25
	Experiment Capsule	26
	Counter	31
	Thermometers	35
	Sample	35
	Experiment and Refrigerator Assembly	38
	Dewars and Refrigerator Magnet	40
	Sample Rotation	41
	Instrumentation	42
V.	EXPERIMENTAL PROCEDURE AND RESULTS	45
	Counting	45
	Temperature Measurement	45
	Vapor pressure	45
	Magnetic susceptibility	46
	Resistance thermometer	49

CHAPTER PAGE

Heat transfer in helium-3 gas 49

Pulse Height Analysis 52

Beta rays 54

Extra pulses 55

Analysis of Angular Distributions 59

Possible P_4 Term 66

VI. DISCUSSION OF RESULTS 68

BIBLIOGRAPHY 73

LIST OF TABLES

TABLE PAGE

I. Energy Levels and Eigenfunctions of the Spin Hamiltonian in Neptunyl Rubidium Nitrate 15

II. Summary of Results 65

LIST OF FIGURES

FIGURE PAGE

1. Decay scheme of neptunium-237, from Strominger, Hollander, and Seaborg, Revs. Modern Phys. 30, 585 (1958) 12
2. Hyperfine energy levels in neptunyl rubidium nitrate 16
3. The alignment parameter G_2 as a function of temperature 18
4. The alignment parameter G_4 as a function of temperature 19
5. Atomic arrangement in uranyl rubidium nitrate 21
6. Schematic diagram of apparatus 27
7. Schematic diagram of experiment capsule 28
8. Photograph of apparatus 29
9. Photograph of sample and associated equipment, removed from the experiment capsule 30
10. Counter voltage-current characteristic 33
11. Counter pulse height as a function of applied bias voltage 34
12. Block diagram of instrumentation 43
13. Susceptibility calibration 47
14. Temperature rise of the resistance thermometer at a power input of 0.02 microwatt 50
15. Typical pulse height distributions at $\theta = 0^{\circ}$ 53

FIGURE PAGE

16. Beta integral counting rate as a function of angle and discrimination level 56

17. Beta integral counting rate (average over θ) as a function of discrimination level 57

18. Integral pulse height distributions 58

19. Angular distributions for Runs 26 and 27, using the data at $77^{\circ}K$ for $V(\theta)$ 61

20. Angular distributions for Runs 19 and 21 62

21. Angular distributions for Runs 20 and 24 63

22. Size of anisotropy as a function of temperature, compared with the normalized theoretical curves of $a_2G_2(T)$ for the two possible sign choices for A and P 67

CHAPTER I

INTRODUCTION

In previous work,[1, 2] the number of alpha particles emitted by neptunium-237 nuclei oriented by the crystalline field in a monocrystalline sample of neptunyl rubidium nitrate was found to be enhanced in the direction perpendicular to the crystalline c axis. This result placed current ideas about the electronic structure of the neptunyl ion in conflict with a simple barrier-penetration picture of alpha-particle emission. The present work was undertaken to clarify the matter.

In this experiment, the nuclear alignment was produced by cooling a sample to a temperature low enough that the hyperfine levels were unequally populated. The hyperfine coupling in neptunyl rubidium nitrate has been determined from paramagnetic resonance experiments by Bleaney, et al.,[3, 4] who expressed their results in terms of a spin Hamiltonian

$$H = AI_zS_z + B(I_xS_x + I_yS_y) + P\left[I_z^2 - \frac{1}{3}I(I + 1)\right] \qquad (1)$$

---

[1] J. W. T. Dabbs, L. D. Roberts, and G. W. Parker, Physica XXIV, S.69 (1958).

[2] L. D. Roberts, J. W. T. Dabbs, and G. W. Parker, Proceedings of the Second International Conference on the Peaceful Uses of Atomic Energy 15, 322 (1958).

[3] B. Bleaney, P. M. Llewellyn, M. H. L. Pryce, and G. R. Hall, Phil. Mag. 45, 992 (1954).

[4] P. M. Llewellyn, thesis, St. John's College (England), 1957, Chap. 4.

with the experimentally determined values,

$$A = \pm 0.16547 \pm 0.00005 \text{ cm}^{-1}$$

$$|B| = 0.01782 \pm 0.00003 \text{ cm}^{-1}$$

$$P = \mp 0.03015 \pm 0.00005 \text{ cm}^{-1}$$

Only the relative sign of A and P was determined experimentally. The upper signs, $A > 0$, $P < 0$, were thought more probable on the basis of a theory of the electronic structure of uranyl-like ions given by Eisenstein and Pryce.[5] In this theory, the bonding electrons of the linear uranyl ion are thought to form a "column of charge" along the oxygen-uranium-oxygen axis. The extra electron in the neptunyl ion probably lies in a $5f_{\phi}$ orbit, as far away as possible from the central charge column, but it has less influence upon the nuclear alignment than the column of charge. The neptunium nucleus, presumably prolate in this region of N and Z,[6] would thus be aligned with its symmetry axis parallel to the oxygen-neptunium-oxygen axis. Since all the neptunyl groups are parallel in this crystal,[7] cooling a monocrystalline sample would align the nuclei parallel to the crystalline c axis.

---

[5] J. C. Eisenstein and M. H. L. Pryce, Proc. Roy. Soc. (London) A229, 20 (1955).

[6] B. R. Mottelson and S. G. Nilsson, Mat. Fys. Skr. Dan. Vid. Selsk. 1, No. 8 (1959).

[7] J. L. Hoard and J. D. Stroupe, cited in G. H. Dieke and A. B. F. Duncan, Spectroscopic Properties of Uranium Compounds (McGraw-Hill Book Co., Inc., New York, 1949), p. 15.

The angular distribution of alpha particles emitted by oriented spheroidal nuclei was predicted by Hill and Wheeler.[8] They pointed out that the potential barrier is both lower and thinner at the "tips" of a prolate nucleus, and that the probability for barrier penetration is a rapidly-varying function of barrier height and thickness. On this basis, and assuming that alpha particles are formed with a probability which is uniform over the nuclear surface, it would be expected that they are emitted preferentially along the nuclear symmetry axis. This prediction, taken together with the direction of nuclear alignment given by Eisenstein and Pryce's theory, led to the result that the alpha-particle emission was expected to be enhanced along the crystalline c axis when a monocrystalline sample was cooled to temperatures comparable to the over-all hyperfine splitting of about 0.65°K. The earlier experimental results were in disagreement with this prediction, and the alpha particles were observed to be emitted preferentially perpendicular to the c axis.

The uneven spacing of the energy levels made it possible to determine unambiguously the signs of the hyperfine coupling constants A and P by studying the alpha-particle anisotropy as a function of temperature over a suitable temperature range. In the present experiment, this was done over the temperature range 0.2-4.2°K.

In Chapter II, the emission of alpha particles from oriented nonspherical nuclei is discussed theoretically both in its nuclear aspects and, more generally, using angular momentum theory. The following chapter

---

[8] D. L. Hill and J. A. Wheeler, Phys. Rev. 89, 1133 (1953).

treats the hyperfine coupling and nuclear alignment in neptunyl rubidium nitrate. The experimental arrangement used is described in detail in Chapter IV, and the data and results are given in Chapter V, together with estimates of errors. Finally, in Chapter VI, the results are discussed and compared to relevant theories.

CHAPTER II

EMISSION OF ALPHA PARTICLES BY ORIENTED NUCLEI

The theory of alpha-particle emission by oriented nuclei may be discussed in terms of a nuclear model. A simple model, which considers only the effect of penetration through a potential barrier, is discussed in Section I. Using a different approach, one can calculate the angular distribution of the alpha particles more generally using the angular momentum formalism. In this treatment, which is given in Section II, the form of the result may be derived without knowledge of the amplitudes and phases of the partial waves, which are left as undetermined constants.

I. NUCLEAR THEORY BASED ON THE BARRIER PENETRATION MODEL

It was first pointed out by Hill and Wheeler[9] that the effect of the potential barrier on alpha-particle emission by non-spherical nuclei would lead to an anisotropic angular distribution of the alpha particles. The barrier penetrability for alpha-particle emission, estimated from a one-dimensional WKB integration, is

$$\exp\left\{-\frac{2}{\hbar}\int_{x_1}^{x_2}[2m(V-E)]^{\frac{1}{2}}dx\right\} \tag{2}$$

where V is the barrier potential and $x_2 - x_1$ is its thickness. This approximate expression predicts that small changes in V with direction will give rise to a large angular anisotropy. For a prolate spheroidal

---

[9] Ibid.

nucleus, the barrier is both lower and thinner at the "tips," so the effect of the variation of barrier penetration with angle would cause the alpha particles to be emitted preferentially along the nuclear symmetry axis. Again, uniform probability of alpha-particle formation has been assumed. This problem has also been studied by Christy,[10] who used a three-dimensional WKB approximation. His calculation predicts a large anisotropy of the same character.

II. ANGULAR MOMENTUM THEORY

A generalized theory of alpha-particle emission from oriented nuclei has been given by Rose.[11] The Hamiltonian for alpha-particle emission is, most generally,

$$H_\alpha = \sum_L \sum_M (-1)^M Y_{L,-M}(\hat{k}) \; T_{LM}(X). \tag{3}$$

Here X stands for all nuclear co-ordinates. The irreducible tensors $T_{LM}(X)$ thus contain all details of alpha-particle formation within the nucleus, barrier penetration, and interactions between the alpha particle and the residual nucleus. The unit vector $\hat{k}$ is directed along the alpha-particle propagation vector $\vec{k}$. The quantum numbers L and M characterize the emitted alpha particle.

---

[10] R. F. Christy, Bull. Am. Phys. Soc. 30, No. 1, 66 (1955).

[11] M. E. Rose, Elementary Theory of Angular Momentum (John Wiley and Sons, Inc., New York, 1957), pp. 176-186. See also J. A. Spiers, Nature 161, 807 (1948).

The angular distribution of the emitted alpha particles is proportional to the transition probability for alpha emission as a function of $\hat{k}$. This is in turn proportional to the square of the matrix element of the Hamiltonian for alpha emission, H_α, averaged over initial states and summed over final states. The angular distribution, W, is thus given by

$$W(\theta, \phi) \propto \sum_f \sum_i g(i) \left| \langle f | H_\alpha | i \rangle \right|^2 \tag{4}$$

where i and f stand for the initial and final states, respectively. The numbers g(i) are the normalized statistical probabilities that the system will be initially in the ith state; they are given by

$$g(i) = \frac{t(i) e^{-E(i)/kT}}{\sum_i t(i) e^{-E(i)/kT}} \tag{5}$$

where E(i) is the energy and t(i) is the statistical weight of the ith state. The energies E(i) are for this case the eigenvalues of the spin Hamiltonian [Equation (1), page 1], and θ is then the angle between the crystalline c axis (z axis in the spin Hamiltonian) and the alpha-particle propagation vector. Because of the "B" term in the spin Hamiltonian, the energy matrix is not diagonal in the representation which diagonalizes I, I_z, and S, S_z. The energy matrix is diagonal in some other representation, with quantum numbers a and b, and eigenfunctions ψ_{ab} which are given by the equation

$$\psi_i = \psi_{ab} = \sum_{m_I m_S} U(ab, m_I m_S) \psi_{I, m_I}(X) \psi_{S, m_S}(e), \tag{6}$$

where the last two factors are the uncoupled wave functions in the nuclear

and electronic spaces, respectively. The unitary matrix U relates the two representations.

In a similar way, the final state may be characterized by quantum numbers c and d, and the final state wave function is

$$\psi_f = \psi_{cd} = \sum_{m_{I'} m_{S'}} V(cd, m_{I'}, m_{S'})\ \psi_{I' m_{I'}}(X)\ \psi_{S' m_{S'}}(e), \tag{7}$$

where the primed quantities refer to the final states.

If the expressions for ψ_i and ψ_f, Equations (6) and (7), are substituted into Equation (4), the angular distribution is then

$$W(\theta,\phi) \propto \sum_{cd} \sum_{ab} g(ab) \sum_{m_I m_S} \sum_{m_{I'} m_{S'}} U(ab, m_I m_S)$$
$$\times V(cd, m_{I'}, m_{X'}) \left| \langle I' m_{I'}, S' m_{S'} | H_\alpha | I m_I S m_S \rangle \right|^2. \tag{8}$$

Since H_α does not operate in the electronic space, the electronic integral is, immediately,

$$\int de\ \psi^*_{S' m_{S'}}\ \psi_{S m_S} = \delta_{SS'}\ \delta_{m_S m_{S'}} \tag{9}$$

When this is applied to Equation (8), and the squared factor expanded, the angular distribution becomes

$$W(\theta,\phi) \propto \sum_{cd} \sum_{ab} g(ab) \sum_{m_S \bar{m}_S} \sum_{m_I \bar{m}_I} \sum_{m_{I'} \bar{m}_{I'}} U(ab, m_I m_S)$$
$$\times U^*(ab, \bar{m}_I \bar{m}_S)\ V(cd, m_{I'}, m_S)\ \ V^*(cd, \bar{m}_{I'}, \bar{m}_S)$$
$$\times \langle I' m_{I'} | H_\alpha | I m_I \rangle \langle I' \bar{m}_{I'} | H_\alpha | I \bar{m}_I \rangle^*. \tag{10}$$

All final states are equally probable, since nuclear spin-lattice relaxation times are long compared to the time for alpha emission. Since V is unitary, the cd sum is then $\delta_{m_{I'} \bar{m}_{I'}}\ \delta_{m_S \bar{m}_S}$.

The matrix elements may be expanded by substitution from Equation (3) and application of the Wigner-Eckart theorem[12] to the irreducible tensors in H_α:

$$\langle I'm_{I'}|H_\alpha|Im_I\rangle = \sum_L \sum_M (-1)^M Y_{L,-M}(\hat{k})$$

$$\times C(ILI';m_I M m_{I'}) \langle I'\|T_L\|I\rangle \quad . \tag{11}$$

The last factor is a reduced matrix element which does not depend upon magnetic quantum numbers. Evaluation of these reduced matrix elements would depend upon the nuclear model which was used, and is not attempted here. The factor $C(ILI';m_I M m_{I'})$ is a Clebsch-Gordon coefficient for the addition of angular momenta.

Since the spin Hamiltonian has cylindrical symmetry, $W(\theta,\phi)$ must be independent of ϕ. The ϕ integral gives $\delta_{m_I \bar{m}_I}$.

By using symmetry relations for Clebsch-Gordon coefficients, expansion series for spherical harmonics, and angular momentum recoupling coefficients, one can reduce the angular distribution to the form

$$W(\phi) = \sum_{LL'} A_{LL'} \sum_\nu G_\nu(T) C(LL'\nu;00) W(IILL';\nu I') P_\nu(\cos\theta) \tag{12}$$

The numbers $A_{LL'}$ give, for $L = L'$, the intensities of the groups of alpha particles with angular momentum L; for $L \neq L'$, they are a measure of interference terms in groups of mixed L. The numbers $W(IILL';\nu I')$ are Racah coefficients for the addition of three angular momenta. The angular distribution is thus expressed as the sum of Legendre polynomials $P_\nu(\cos\theta)$. The coefficient $C(LL'\nu;00)$ is zero unless $L + L' + \nu$ is an

---

[12] *Ibid.*, p. 85.

even integer. Since parity is assumed to be conserved, L and L' are either both odd or both even, depending on the spins and parities of the initial and residual nuclei, and υ must be even or zero. The maximum value of υ must be less than L + L', from $C(LL'\upsilon;00)$ in Equation (12), and also less than 2I, from $C(I\upsilon I;m_I 0)$ in Equation (13) below.

The quantities $G_\upsilon(T)$ are given by

$$G_\upsilon(T) = \sum_{ab} g(ab) \sum_{m_I m_S} U(ab,m_I m_S)^2 \, C(I\upsilon I;m_I 0) \tag{13}$$

and they contain all of the alignment information; the variation of g(ab) with temperature gives the variation of alpha-particle angular distribution with temperature. In accordance with the Wigner-Eckart theorem, the Clebsch-Gordon coefficient may be thought of as the matrix element of an operator with unity reduced matrix element; thus

$$C(I\upsilon I;m_I 0) = \langle Im_I | T_{\upsilon 0} | Im_I \rangle . \tag{14}$$

The operators $T_{\upsilon 0}$ are elements of irreducible tensors of rank υ; for υ = 0, 2, and 4 they are given by

$$T_{00} = \sqrt{2I + 1} \tag{15a}$$

$$T_{20} = \sqrt{\frac{180\,(2I - 2)!}{(2I + 3)!}} \left[I_z^2 - \tfrac{1}{3} I(I + 1) \right] \tag{15b}$$

$$T_{40} = 210 \sqrt{\frac{(2I - 4)!}{(2I + 5)!}} \left\{ I_z^4 - \tfrac{1}{15} \left[3I^2(I + 1)^2 - I(I + 1) \right] - \tfrac{1}{7} \left[6I(I + 1) - 5 \right] \left[I_z^2 - \tfrac{1}{3} I(I + 1) \right] \right\} \tag{15c}$$

The decay scheme of neptunium-237, as given in the review of Strominger, Hollander, and Seaborg,[13] is shown in Figure 1. Too little is known about the spins and parities of the levels in protoactinium-233 to permit a detailed analysis of the angular momenta of the various alpha groups. Since the spin of neptunium-237 is $I = \frac{5}{2}$,[14] the maximum allowable value for ν is 4, and the angular distribution can involve only Po, P_2 and P_4, with the form

$$W(\theta) = 1 + a_2G_2(T)P_2(\cos\theta) + a_4G_4(T)P_4(\cos\theta), \tag{16}$$

where the coefficients a_2 and a_4 are unknown combinations of reduced nuclear matrix elements, Clebsch-Gordon coefficients, and Racah coefficients.

Geometry correction. The observed angular distribution will differ from $W(\theta)$ because of the finite size of both source and counter. For a circular uniformly illuminated source and a counter whose sensitivity is symmetric, Rose has shown[15] that if the true angular distribution is

$$W(\theta) = 1 + \sum_{\nu \neq 0} B_\nu P_\nu(\cos\theta), \tag{17}$$

then the observed angular distribution will be approximately equal to

---

[13] D. Strominger, J. M. Hollander, and G. T. Seaborg, Revs. Modern Phys. 30, 585 (1958).

[14] K. L. Vander Sluis and J. R. McNally, Jr., J. Opt. Soc. Am. 44, 87 (1954).

[15] M. E. Rose, ORNL-2050 (1956) (unpublished).

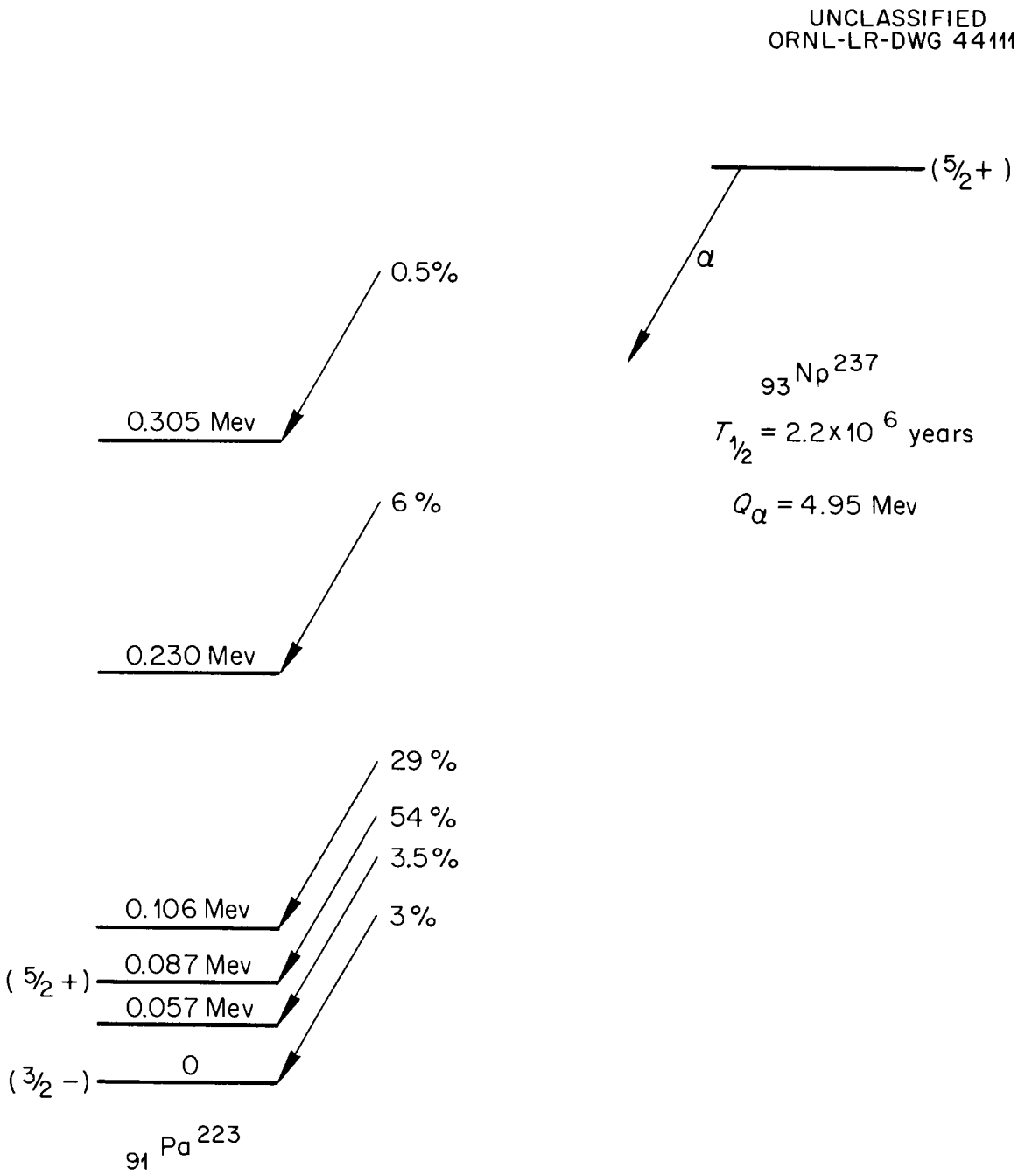

Figure 1. Decay scheme of neptunium-237, from Strominger, Hollander, and Seaborg, Revs. Modern Phys. 30, 585 (1958).

$$W(\theta) \approx 1 + \sum_{\nu \neq 0} B_\nu \left\{ 1 - \frac{\lambda}{4} K_0^{(2)} + \frac{\lambda^2 + 34\lambda}{64} K_0^{(4)} - \frac{3}{8}\lambda \left[K_0^{(2)} \right]^2 \right\} P_\nu(\cos\theta)$$

$$\approx 1 + \sum_{\nu \neq 0} b_\nu B_\nu P_\nu(\cos\theta), \tag{18}$$

where

$\lambda = \nu(\nu + 1)$

$K_0^{(2)} = (r_1^{\,2} + r_2^{\,2})/2L^2$

$K_0^{(4)} = (\frac{1}{3}r_1^{\,4} + \frac{1}{3}r_2^{\,4} + r_1^{\,2}r_2^{\,2})/L^4$

r_1 = radius of source

r_2 = radius of counter

L = distance from source to counter.

The only change is a multiplying factor b_ν for each component in the original angular distribution. For this experiment, $r_1 = 0.42$ cm, $r_2 = 0.48$ cm, and $L = 2.0$ cm. The multiplying factor for the P_2 term is $b_2 = 0.93$; for the P_4 term it is $b_4 = 0.80$.

Although the assumptions on which this geometry correction is based are only qualitatively fulfilled for this experiment, the calculation is thought to be a fair estimate of the necessary correction.

CHAPTER III

NUCLEAR ALIGNMENT IN NEPTUNYL RUBIDIUM NITRATE

Llewellyn has studied[16, 17] the microwave paramagnetic resonance spectrum of neptunyl rubidium nitrate at 13°K. He found that the results were consistent with a spin Hamiltonian

$$H = g_{\parallel}\,\beta H_z I_z + g_{\perp}\beta(H_x I_x + H_y I_y) + A I_z S_z + B(I_x S_x + I_y S_y) + P\left[I_z^2 - \tfrac{1}{3}I(I+1)\right], \tag{19}$$

with the following parameters

$g_{\parallel} = 3.405 \pm 0.008$

$g_{\perp} = 0.205 \pm 0.006$

$\gamma = \pm 2.4 \pm 0.6$

$A = \mp 0.16547 \pm 0.00005\ \mathrm{cm}^{-1} = \mp 0.23801^{\circ}\mathrm{K}$

$|B| = 0.01782 \pm 0.00003\ \mathrm{cm}^{-1} = 0.02563^{\circ}\mathrm{K}$

$P = \pm 0.03015 \pm 0.00005\ \mathrm{cm}^{-1} = \pm 0.04337^{\circ}\mathrm{K}.$

The energy levels and eigenfunctions of this experimentally determined spin Hamiltonian in zero external magnetic field are given in Table I and shown in Figure 2, for the sign choice $A < 0$, $P > 0$. For the other sign choice ($A > 0$, $P < 0$), the figure should be inverted. Of particular interest is the "B" term, which admixes states of equal K ($K = m_I + m_S$), and removes the degeneracy of the state in which $K = 0$.

---

[16] Bleaney, Llewellyn, Pryce, and Hall, loc. cit.

[17] Llewellyn, loc. cit.

TABLE I

ENERGY LEVELS AND EIGENFUNCTIONS OF THE SPIN HAMILTONIAN IN NEPTUNYL RUBIDIUM NITRATE[a]

Level Number	m_I [b]	m_S [b]	K [b]	$E-E_0$ [c] (^oK)	$E-E_1$ (^oK)	Eigenfunction[d]	Degeneracy
1	$\pm\frac{3}{2}$	$\pm\frac{1}{2}$	±2	-0.20867	0	$0.9991\ \psi(\pm\frac{3}{2},\pm\frac{1}{2}) + 0.0440\ \psi(\pm\frac{5}{2},\mp\frac{1}{2})$	2
2	$\pm\frac{1}{2}$	$\pm\frac{1}{2}$	±1	-0.17915	0.02952	$0.9939\ \psi(\pm\frac{1}{2},\pm\frac{1}{2}) + 0.1096\ \psi(\pm\frac{3}{2},\mp\frac{1}{2})$	2
3	$\pm\frac{5}{2}$	$\pm\frac{1}{2}$	±3	-0.15294	0.05573	$\psi(\pm\frac{5}{2},\pm\frac{1}{2})$	2
4	$\pm\frac{1}{2}$	$\mp\frac{1}{2}$	0	-0.09459	0.11408	$\psi(\pm\frac{1}{2},\mp\frac{1}{2})$	1
5	$\pm\frac{1}{2}$	$\mp\frac{1}{2}$	0	-0.01771	0.19096	$\psi(\pm\frac{1}{2},\mp\frac{1}{2})$	1
6	$\pm\frac{3}{2}$	$\mp\frac{1}{2}$	±1	+0.15359	0.36226	$0.0039\ \psi(\pm\frac{3}{2},\mp\frac{1}{2}) + 0.1096\ \psi(\pm\frac{1}{2},\pm\frac{1}{2})$	2
7	$\pm\frac{5}{2}$	$\mp\frac{1}{2}$	±2	+0.44333	0.65200	$0.0001\ \psi(\pm\frac{5}{2},\mp\frac{1}{2}) + 0.0440\ \psi(\pm\frac{3}{2},\pm\frac{1}{2})$	2

[a]Calculated from the spin Hamiltonian, Equation (1).

[b]The quantum numbers m_I and m_S are only approximately constants of the motion; the quantum number $K \equiv m_I + m_S$ is a constant.

[c]E_0 is the unperturbed, 12-fold degenerate, ground-state energy.

[d]The decoupled wave functions are $\psi(m_I,m_S)$.

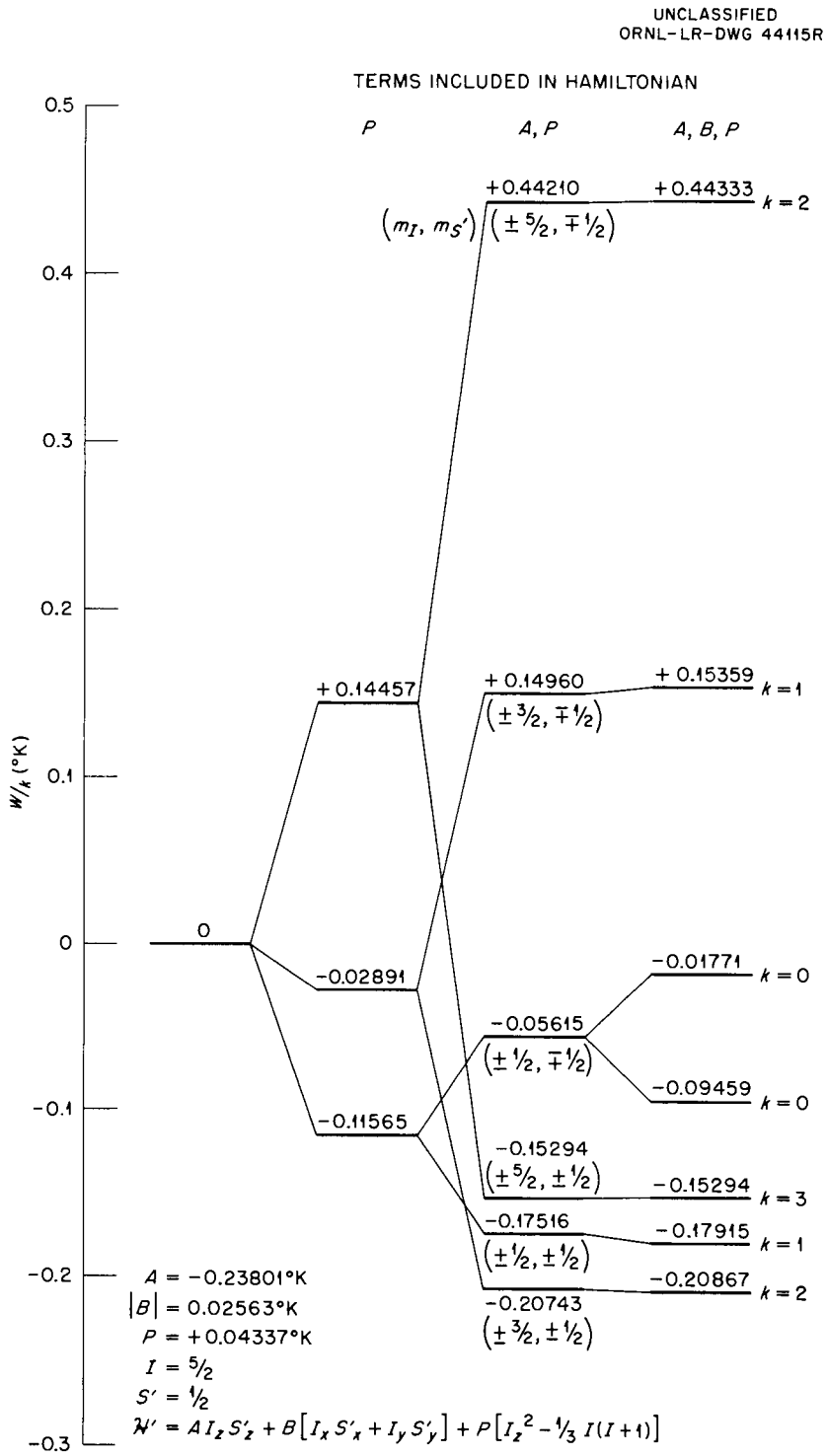

Figure 2. Hyperfine energy levels in neptunyl rubidium nitrate.

The energy levels given in Table I and shown in Figure 2 have been used to calculate the alignment parameters $G_2(T)$ and $G_4(T)$, which are shown as a function of temperature in Figures 3 and 4, for both choices of the signs of A and P. These values of G_2 and G_4 are thus derived directly from the experimentally determined values of the hyperfine coupling constants. In Figure 3, the ordinate is $\left| a_2G_2(T) \right|$, normalized so $\left| a_2G_2(1.16^{\circ}K) \right| = 0.0634$. This value was determined in earlier measurements.[18, 19]

Also in earlier work,[20] the magnetic susceptibility of samples of pure neptunyl rubidium nitrate was measured over the temperature range 1.2 - 4.2°K. This was done to confirm, at least insofar as the g factors are concerned, that the Hamiltonian obtained from microwave data at 13°K and 20°K is valid at lower temperatures. Also, since the microwave work used a dilute sample, it was of interest to examine a pure sample. The susceptibility results for a 7.8 g powder sample gave $g_{\parallel}^2 + 2g_{\perp}^2 = 11.26 \pm 0.1$, in good agreement with the result from microwave data of 11.64 ± 0.3. The susceptibility of a single crystal sample weighing 3.3 g was measured to be $g_{\parallel} = 3.45 \pm 0.07$, which agrees with the microwave value of 3.405 ± 0.008. The small measured Weiss constant of 0.04°K

---

[18] Dabbs, Roberts, and Parker, loc. cit.

[19] Roberts, Dabbs, and Parker, loc. cit.

[20] J. W. T. Dabbs, L. D. Roberts, and G. W. Parker, Bull. Am. Phys. Soc. II, 2, 185 (1957).

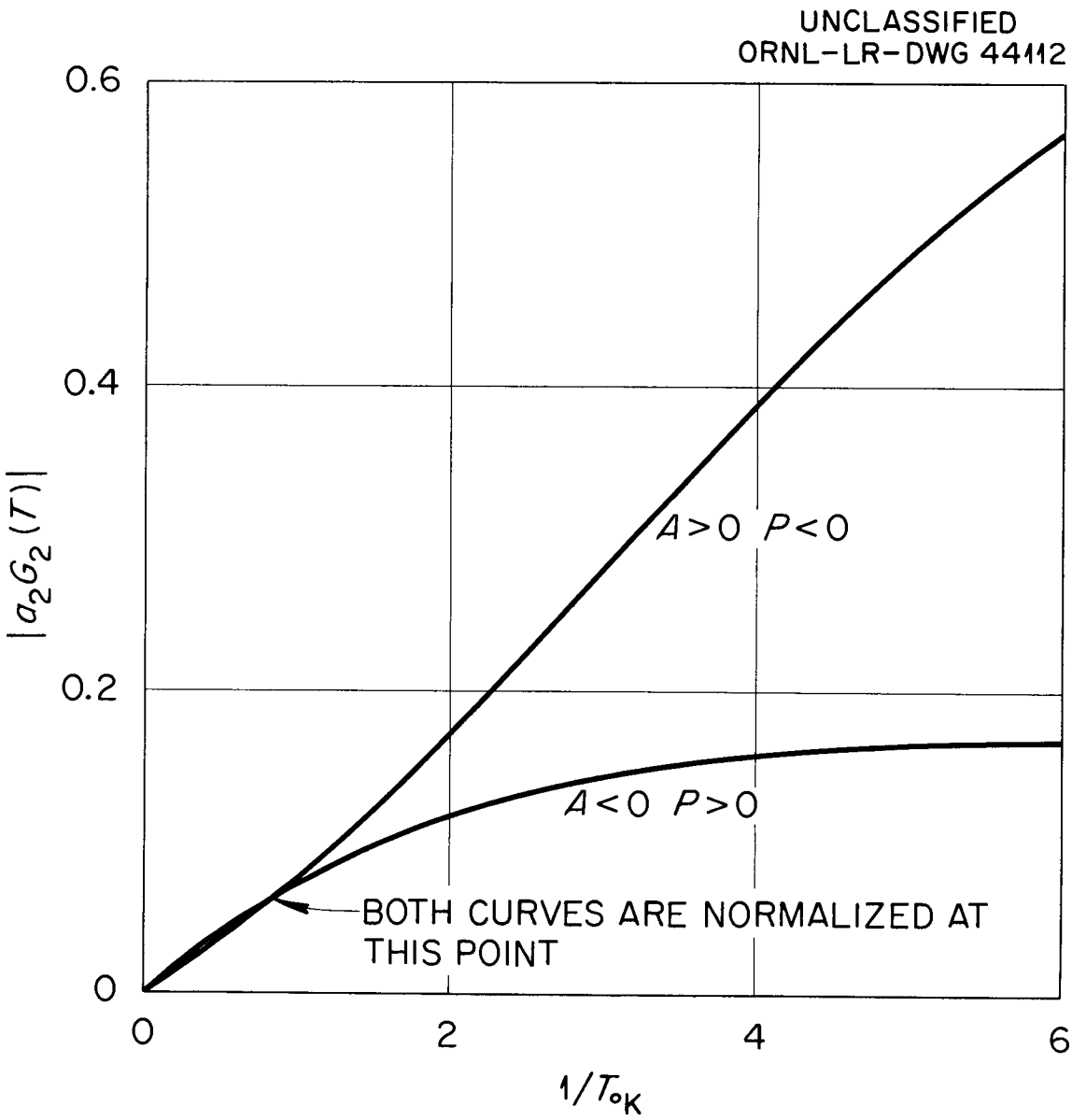

Figure 3. The alignment parameter G_2 as a function of temperature, normalized so that $a_2G_2(T) = 0.0634$ at $T = 1.16°K$.

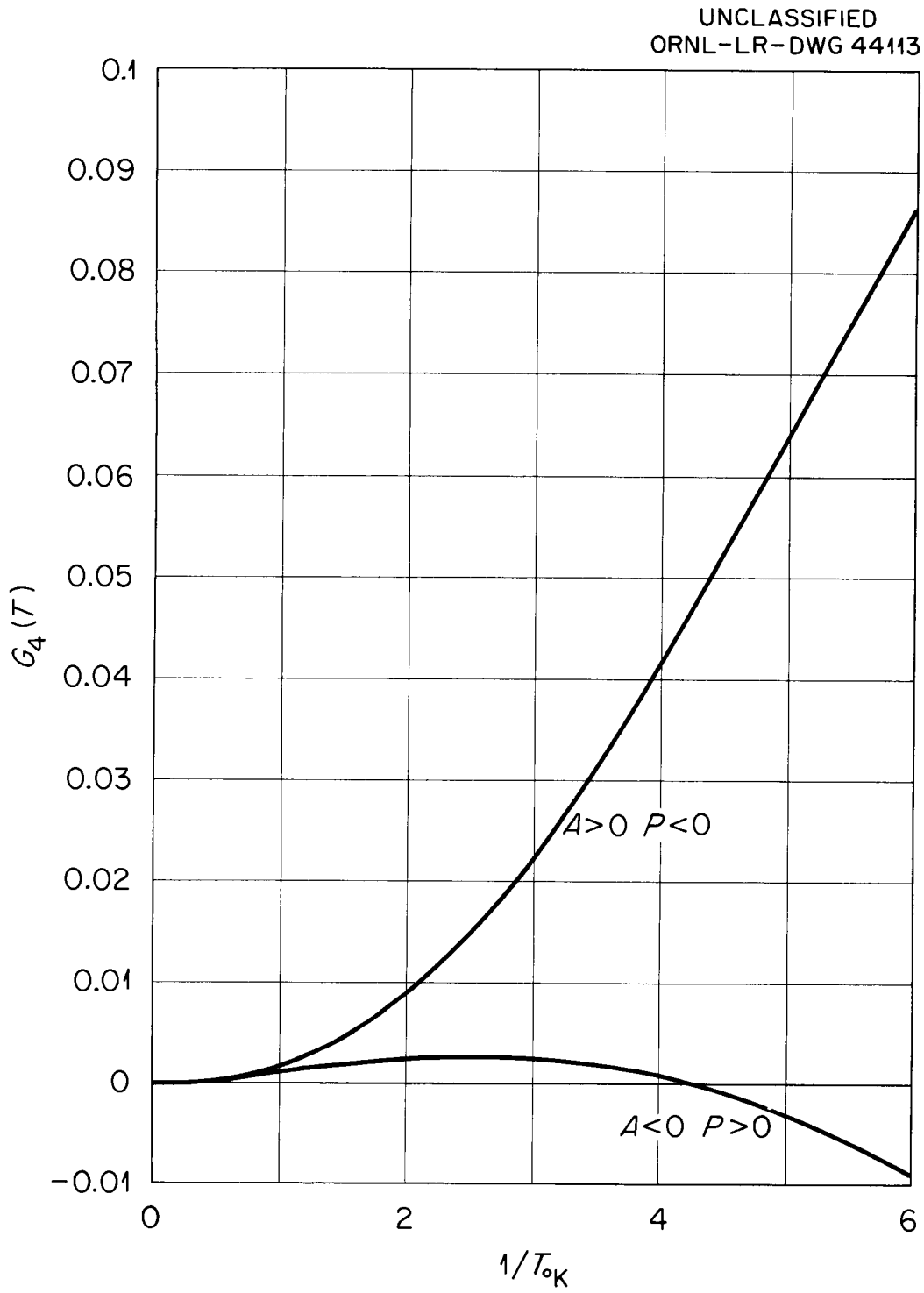

Figure 4. The alignment parameter G_4 as a function of temperature.

suggests that the spin Hamiltonian is valid down to temperatures of the order of $0.1^{\circ}K$.

From the observed line width in the paramagnetic resonance experiments, Llewellyn[21] inferred that the spin-lattice relaxation time was short at $13^{\circ}K$. No effect of a relaxation time was observed during the course of the measurements on magnetic susceptibility[22] at temperatures as low as $1.2^{\circ}K$, or in the course of these experiments in the temperature range $0.2 - 4.2^{\circ}K$.

The crystal structure of uranyl rubidium nitrate has been studied by Hoard and Stroupe,[23] and the atomic arrangement is shown in Figure 5, which has been taken from their work. The linear uranyl groups all lie parallel to the c axis of the crystal, each surrounded by three nitrate groups in the equatorial plane. The U-O distance in the $(UO_2)^{++}$ ion was estimated by Hoard and Stroupe to be 1.58 Å; Zachariasen[24] has suggested a value of 1.63 Å, based on an empirical correlation of bond length and bond strength in $(XO_2)^{++}$ ions. This is in any case very much smaller than the distance (≈2.7 Å) between the uranium atom and its next nearest neighbors, the six oxygen atoms in the NO_3 groups. Neptunyl rubidium nitrate is known to be isostructural with the uranyl compound, so the

---

[21] Llewellyn, loc. cit.

[22] J. W. T. Dabbs, L. D. Roberts, and G. W. Parker, Bull Am. Phys. Soc. II, 2, 185 (1957).

[23] Hoard and Stroupe, loc. cit.

[24] W. H. Zachariasen, Acta Cryst. 7, 795 (1954).

UNCLASSIFIED
ORNL-LR-DWG 45533

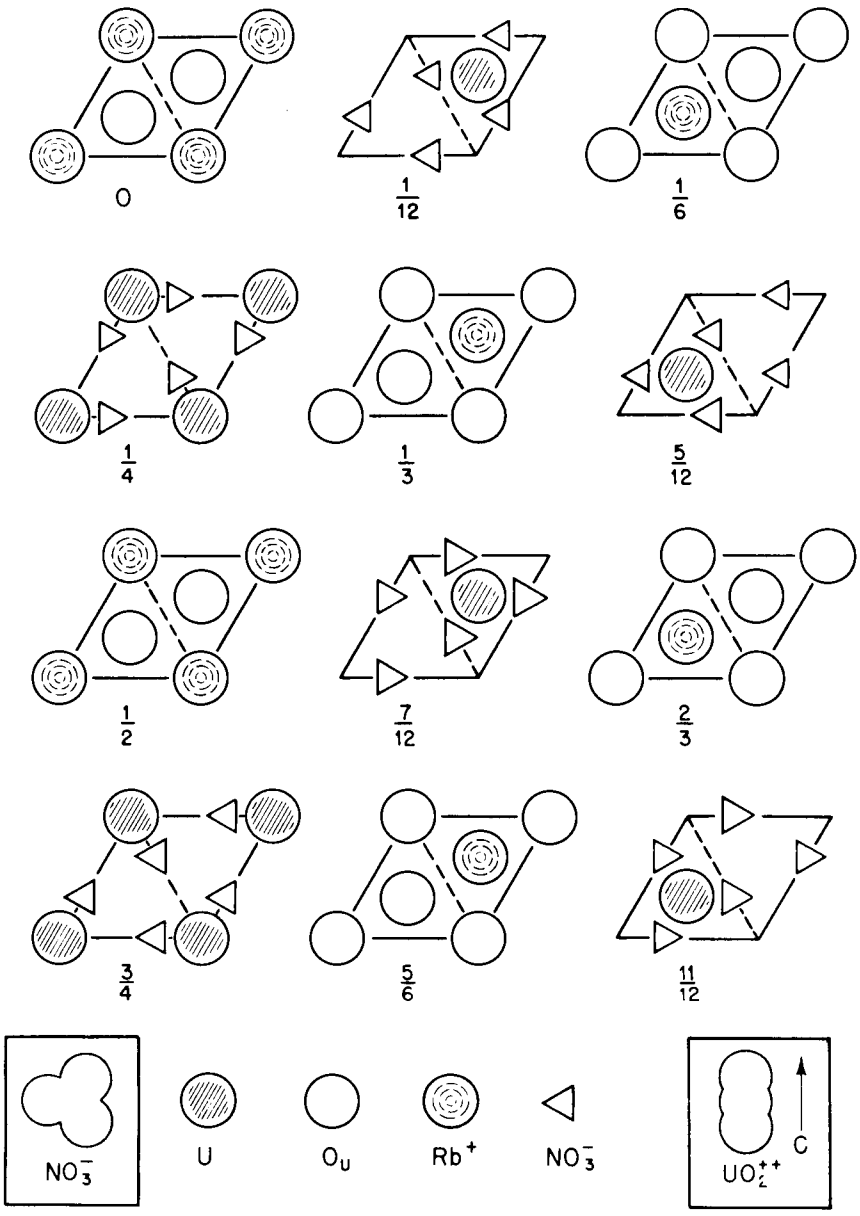

Figure 5. Atomic arrangement in uranyl rubidium nitrate. The atoms are drawn approximately to scale; the numbers are displacements along the crystalline c axis, expressed as fractions of the lattice period. This drawing was reproduced from Hoard and Stroupe, loc. cit.

atoms in the $(NpO_2)^{++}$ ion may be assumed to have essentially the same locations as those in $(UO_2)^{++}$.

Eisenstein and Pryce[25] have given a theory of the electronic structure and magnetic properties of uranyl-like ions. In uranyl, two of the six uranium electrons outside the radon core have been lost, and the remaining four are used to form covalent bonds with the oxygen atoms. The electronic states are expected to be hybrids of the available states 5f, 6d, 7s, and perhaps 7p. In the simplest model, all bonding orbital states have $m_\ell = 0$ (σ bonding), and "the electronic charge cloud of the bonding electrons is axially symmetrical and heavily concentrated in a column around the axis.[26] Two of the bonding electrons are in $5f_\sigma$ states, and the other two, in hybrid $6d_\sigma$ - 7s states.

The chemical and structural similarity of $(NpO_2)^{++}$ to $(UO_2)^{++}$ suggests that they have the same bond structure, and that the extra electron of $(NpO_2)^{++}$ goes into a $5f_\phi$ orbit ($m_\ell = \pm 3$), as far away as possible from the central charge column.

On this basis of this model, Eisenstein and Pryce calculated theoretical expressions for the hyperfine coupling constants A, B, and P. The results of their original calculations are as follows:

$$A = +2\gamma\beta\beta_n \langle r^{-3} \rangle_{5f} \left[\frac{20}{3} + \frac{2}{3}\sqrt{6}q + 4q^2 + K(1 + p^2 - q^2) \right] \times (1 + p^2 + q^2)^{-1} \qquad (20)$$

---

[25] Eisenstein and Pryce, loc. cit.

[26] Ibid., p. 23.

$$B = 2\gamma\beta\beta_n \langle r^{-3} \rangle_{5f} \left[\frac{2}{3} - \frac{5}{3}\sqrt{6q} - 2K \right] (1 + p^2 + q^2)^{-1} \tag{21}$$

$$P = -\frac{3e^2Q}{4I(2I-1)} \left[\left(\frac{16}{15}\alpha - \frac{2}{3} \right) \langle r^{-3} \rangle_{5f} + \frac{8}{7}\alpha' \langle r^{-3} \rangle_{6d} \right] \tag{22}$$

Q = nuclear quadrupole moment

γ = nuclear gyromagnetic ratio (units of $e/2Mc$)

β = Bohr magneton

β_n = nuclear magneton

p = admixture of $5f_\phi(j_z = \pm \frac{7}{2})$ into $5f_\phi(j_z = \pm\frac{5}{2})$ ground-state doublet, caused by $V_6{}^6$ crystal field; $p \approx 0.069$

q = admixture of $5f_\delta(j_z = \pm\frac{5}{2})$ into $5f_\phi(j_z = \pm\frac{5}{2})$ caused by spin-orbit interaction; $q \approx 0.2$

K = non-dimensional parameter giving the effect of unpaired spin density at the nucleus (unpaired s-electron effect); $K \approx 0.7$

α = probability that a 5f bonding electron is in the neptunium state, rather than on the oxygen atom; $\alpha \approx 0.5$

α' = probability that a 6d bonding electron is in the neptunium state, rather than on the oxygen atom; $\alpha' < 0.5$.

The numerical estimates were given by Llewellyn,[27] who also estimated that $\langle r^{-3} \rangle_{5f} = 30\text{Å}^{-3}$ and $\langle r^{-3} \rangle_{6d} \approx 75\text{Å}^{-3}$. These values of the parameters gave satisfactory agreement between the theoretical values and the experimentally determined magnitudes of the g-factors and the hyperfine coupling constants.

---

[27] Llewellyn, loc. cit.

Since neptunium-237 has an odd number of protons, its magnetic dipole moment is expected to be positive ($\gamma > 0$), and the theory in its original form predicted $A > 0$. The microwave paramagnetic resonance experiments showed that A and P are of opposite signs, so on this basis, $P < 0$. This was in accord with the expected positive quadrupole moment, Q, of neptunium-237, and with Equation (22), which requires P to be of opposite sign to Q.

Since the alpha-particle experimental results reported here have been obtained, Pryce[28] has pointed out an error in these calculations. Except in very simple systems, the effective electron angular momentum, S, is not truly the resultant of the spins of the valence electrons, but rather it is some fictitious spin operator, chosen so that the multiplicity of the ground state of the ion may be set equal to $2S + 1$. In a system with two states (orbital singlet), the basic states are the eigenstates for $S_z = \pm\frac{1}{2}$. If the axis of quantization is also an axis of cylindrical symmetry, then only one of the two possible choices of basic states will be available, since interchanging the two destroys the symmetry. In their original paper, Eisenstein and Pryce[29] neglected this point, and chose the basic states incorrectly. The corrected results of this theory now predict $A < 0$, $P > 0$, but the theory still requires P to be of opposite sign to Q.

---

[28] M. H. L. Pryce, Phys. Rev. Letters 3, 375 (1959).

[29] Eisenstein and Pryce, loc. cit.

CHAPTER IV

EXPERIMENTAL ARRANGEMENT

In an early attempt to make this measurement, a monocrystalline sample was mounted mechanically in contact with a paramagnetic salt for cooling. The alpha particles were counted at a fixed angle as a function of temperature in the region below $1^{\circ}K$, the change in counting rate at a known angle being a measure of the anisotropy of alpha-particle emission. The results of that experiment were consistent with the results reported here, but their validity was doubted because it was not possible to determine reliably the temperature of the surface of the sample crystal. Accordingly, the experiment described here was designed to cool the crystal surface with helium-3 gas, which has an appreciable vapor pressure[30]--and hence thermal conductivity--even at $0.2^{\circ}K$. Since the low-temperature ($< 1^{\circ}K$) parts of the equipment had to be thermally isolated, the entire alpha-particle experiment was located within an isothermal enclosure filled with helium-3 gas. This enclosure contained the rotatable sample, the alpha counter, the rotation indicators, and a resistance thermometer, and was in thermal contact with a paramagnetic salt which could be cooled by adiabatic demagnetization. This assembly was mounted on cotton threads in a vacuum enclosure inside dewar vessels

---

[30] E. F. Hammel, in C. J. Gorter (ed.), Progress in Low Temperature Physics (North-Holland Publishing Co., Amsterdam, 1955), I, 84.

for liquid nitrogen and liquid helium. The experimental data were the observed alpha-particle counting rates as a function of the temperature and of the angle θ between the crystalline c axis and a line joining the sample and the counter. Schematic diagrams of the experimental apparatus are shown in Figures 6 and 7, and photographs of it are shown in Figures 8 and 9.

I. EXPERIMENT CAPSULE

The basic experiment was housed entirely within a cylindrical copper container 9.5 cm long and 4.1 cm in diameter, shown schematically in Figure 6. The sample in its holder was located here, attached to a vertical shaft mounted in small ball bearings so the sample could be rotated. The sample was mounted with the crystalline c axis horizontal, perpendicular to the axis of rotation. The interaction of a small permanent magnet, mounted on the sample holder, with external, rotatable, Helmholtz coils, provided the force to rotate the sample assembly and to hold it at any desired angle. Measurement of the capacitance of an assembly of fixed and rotating condenser plates furnished a means of determining the angular position of the sample. Fixed stops at angles of exactly 0° and 90° were electrically insulated, so that an electrical continuity check could determine that the sample was actually at these angles.

A heater of manganin wire in thermal contact with the capsule provided means for increasing its temperature while the experiment and refrigerator assembly was thermally isolated.

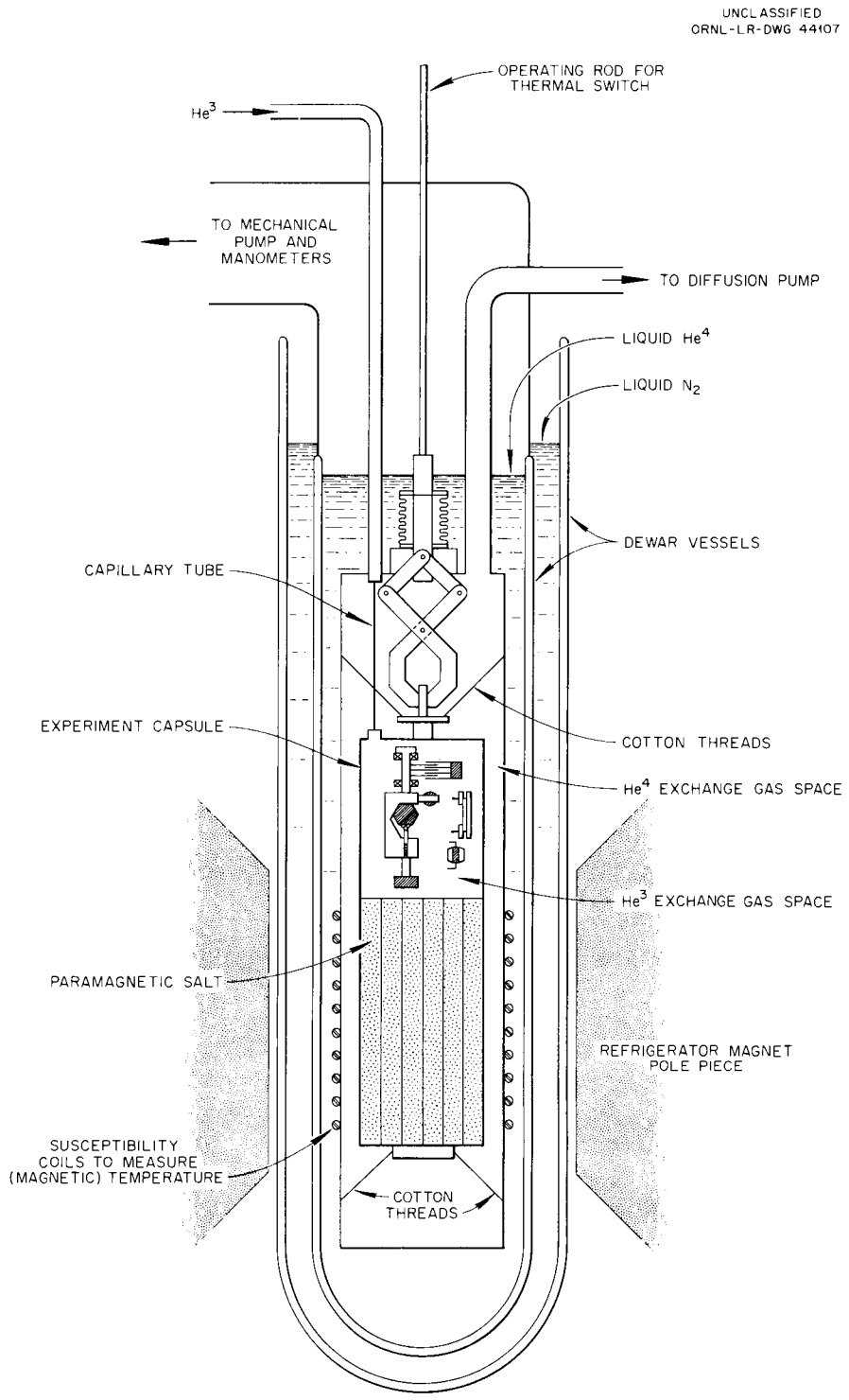

Figure 6. Schematic diagram of apparatus.

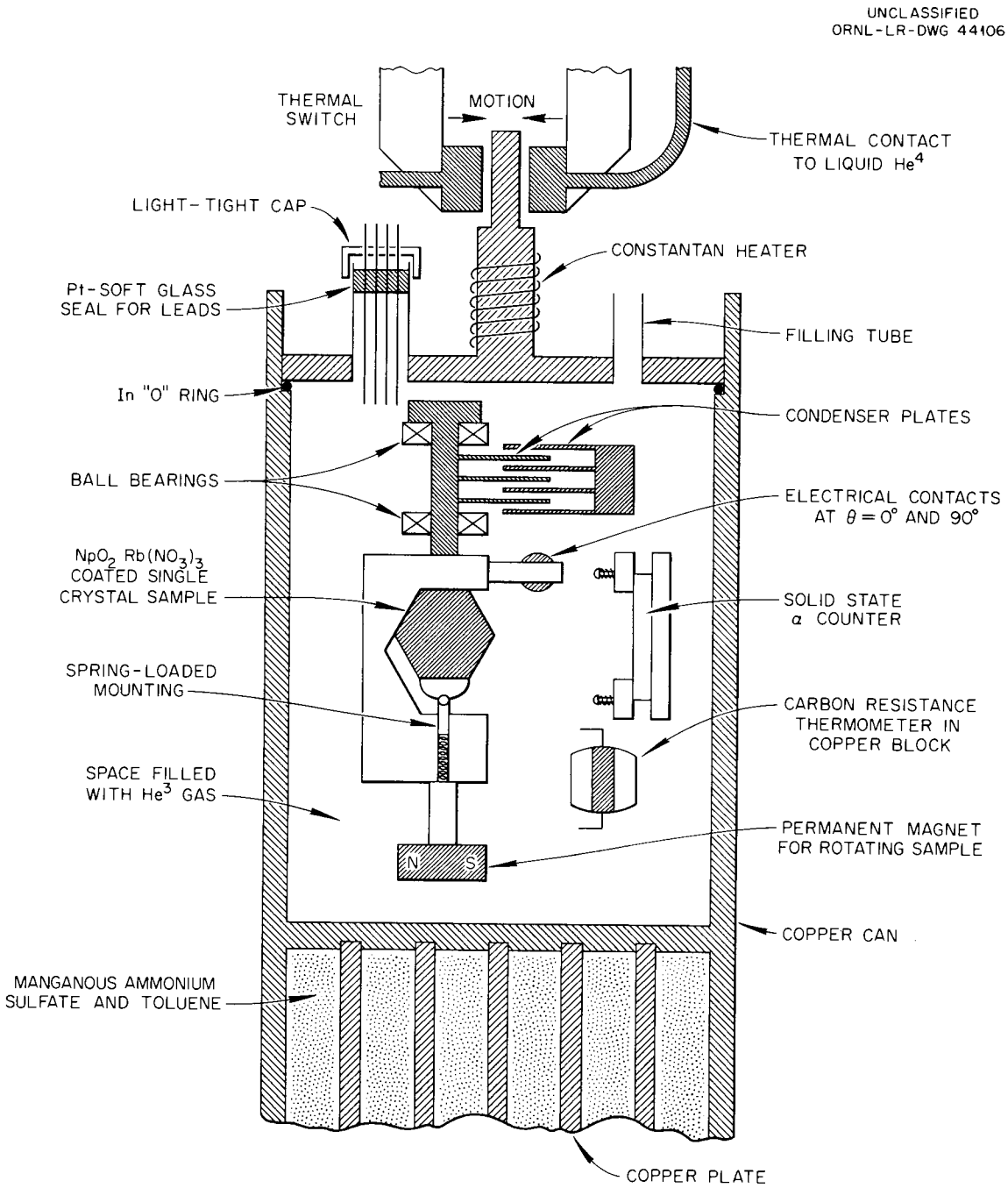

Figure 7. Schematic diagram of experiment capsule.

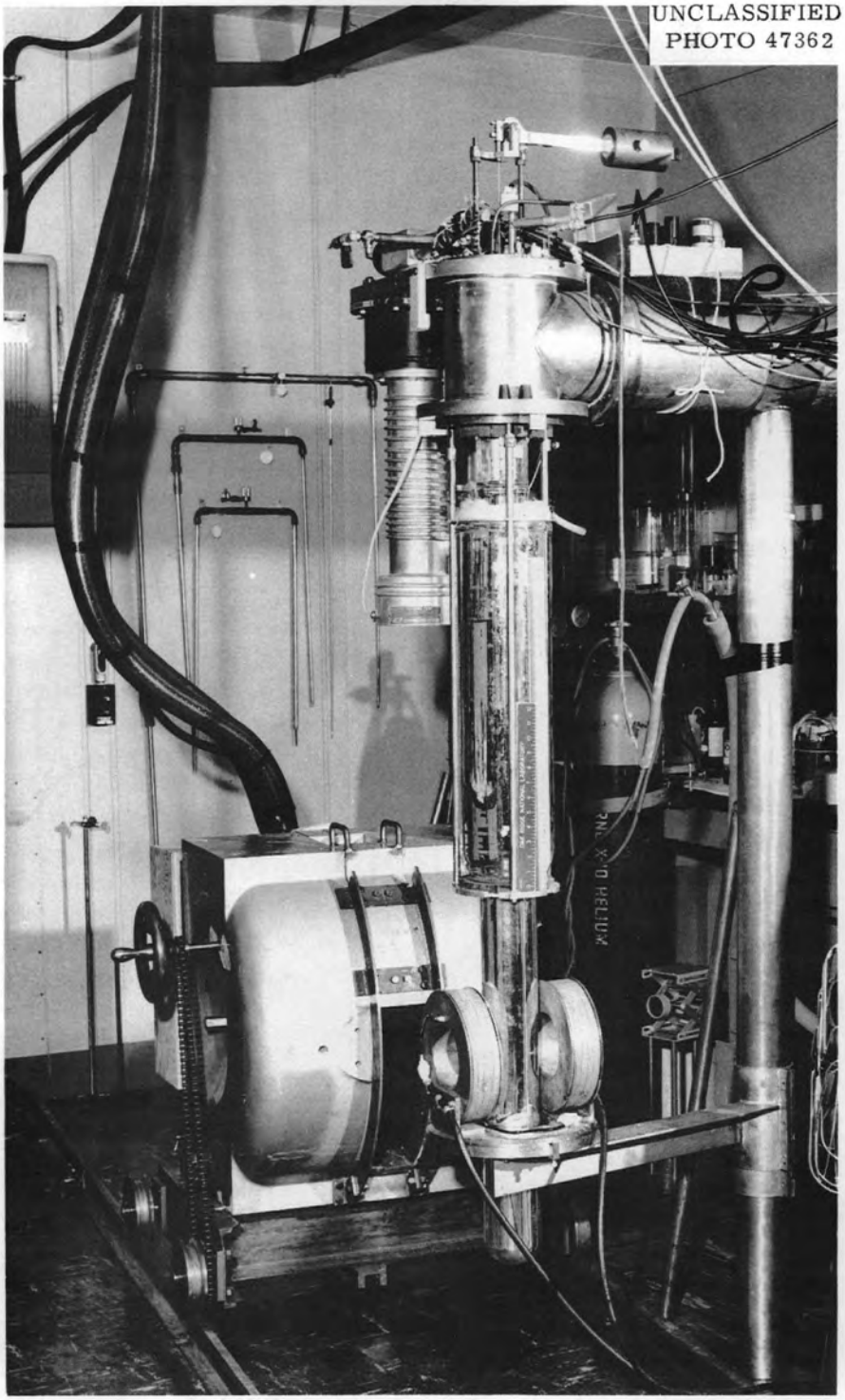

Figure 8. Photograph of apparatus.

UNCLASSIFIED
PHOTO 47357

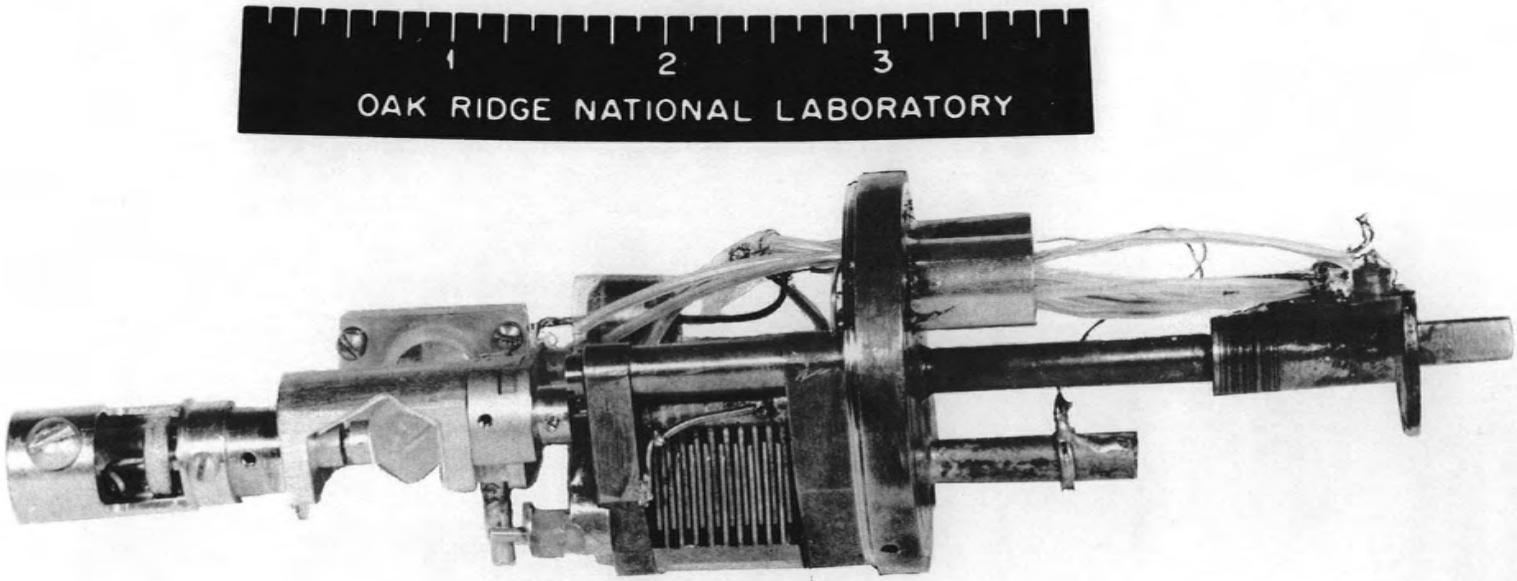

Figure 9. Photograph of sample and associated equipment, removed from the experiment capsule.

Counter. The alpha particles were counted by a germanium surface barrier counter developed by F. J. Walter, et al.[31] This counter was made from a piece of pure germanium 1 cm x 1 cm x 0.045 cm. The surfaces were lapped and etched, and gold was evaporated onto the two flat faces only. Walter, et al., have given a theory of operation of these counters. At the surface of the germanium, the band structure is altered by the presence of surface states, and a large equilibrium voltage gradient can exist there. The slope and depth of this voltage gradient can be increased by impressing a suitable bias voltage across the counter. An alpha particle striking the counter will produce an electron-hole pair for each 3 ev which it loses within the germanium; if these charge carriers are within the region of high voltage gradient, or if they can diffuse into it, their motion through the potential difference will induce an electrical signal pulse which is proportional to the total charge collected, and inversely proportional to the total capacitance of the counter and the amplifier input circuit.

At 77°K, the bulk resistivity of the germanium is sufficiently low that appreciable voltage gradients can exist only within the barrier region, estimated for the counter used to be 10^{-3} cm thick. This is comparable to the range of 4.8 Mev alpha particles in germanium.[32] The effective capacitance of the counter is then just the capacitance of the barrier region, which is high because the barrier is thin. At 77°K, the

---

[31] F. J. Walter, J. W. T. Dabbs, and L. D. Roberts, ORNL-2877 (1960) (unpublished).

[32] W. H. Brattain and G. L. Pearson, Phys. Rev. 80, 846 (1950).

measured capacitance of the counter used was 600 pf (1 pf = 10^{-12} f).

At 4.2°K and below, the intrinsic resistivity of purified germanium is very high.[33] The applied voltage produces a gradient across the entire counter, and the barrier plays a less important role in pulse formation. The effective thickness is now the entire physical thickness of the germanium wafer, and the effective capacitance of the counter was correspondingly reduced at 4.2°K and below, to less than 100 pf, including the stray and lead capacitances. The observed alpha-particle pulse height was therefore larger at 4.2°K than at 77°K by the ratio of the capacitances. In the case of a particle whose range in germanium is large compared to the barrier thickness, the ratio of the observed pulse height at 4.2°K to that observed at 77°K, is even larger than the capacitance ratio, since the long-range particle can lose more energy within the larger effective thickness of the counter.

The characteristics of this counter were measured in collaboration with F. J. Walter. In Figure 10 is shown the voltage-current curve observed at 77°K. There was evidently a barrier on both faces; the one for negative applied voltage (front face) showed breakdown at higher voltage than the one for positive applied voltage (back face). The observed pulse height is shown as a function of applied voltage in Figure 11.

The counter was tested for the effect of a magnetic field. A field of 160 gauss (the field produced by the Helmholtz coils with 20

---

[33] S. H. Koenig and G. R. Gunther-Mohr, J. Phys. Chem. Solids 2, 268 (1957).

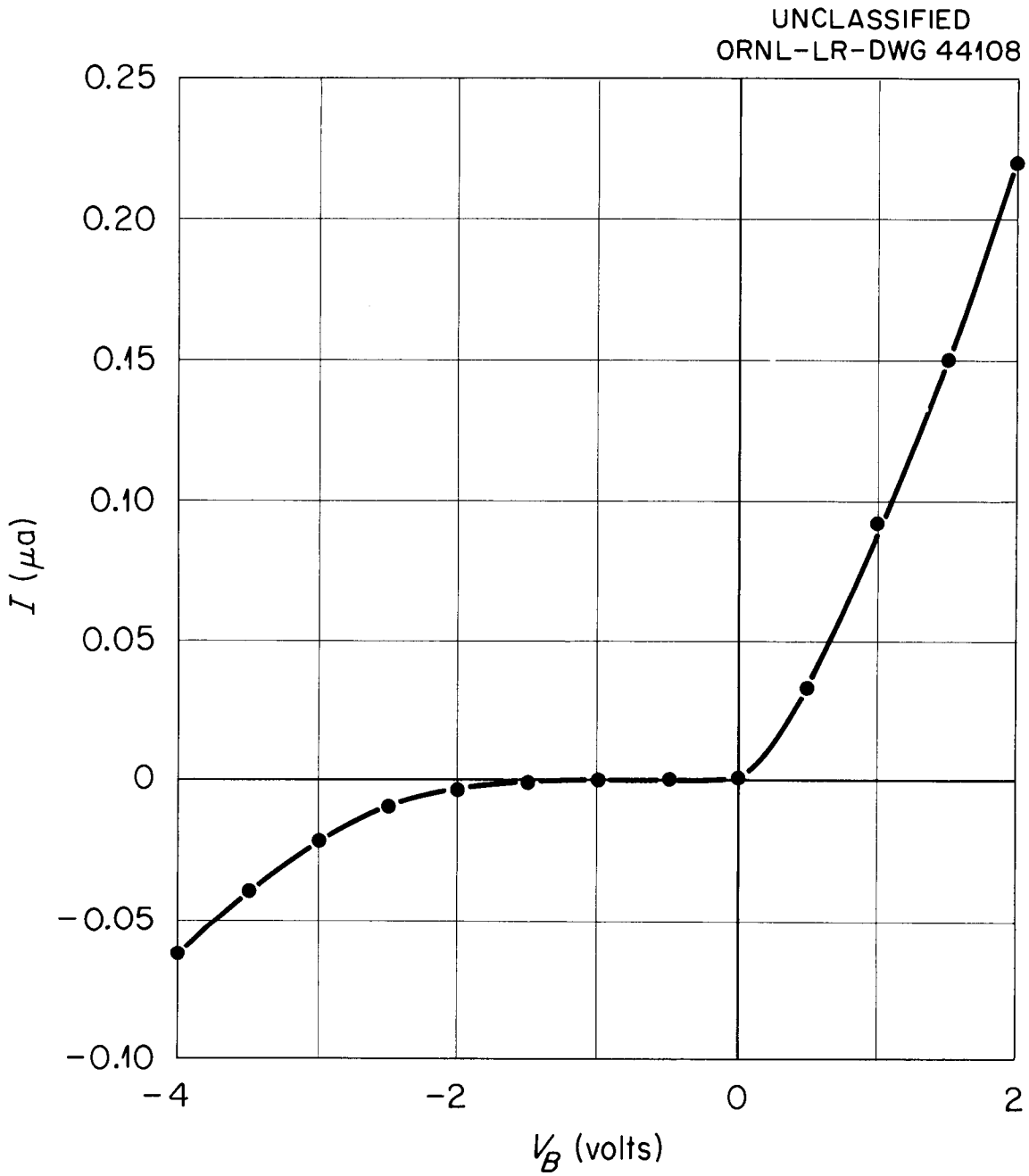

Figure 10. Counter voltage-current characteristic.

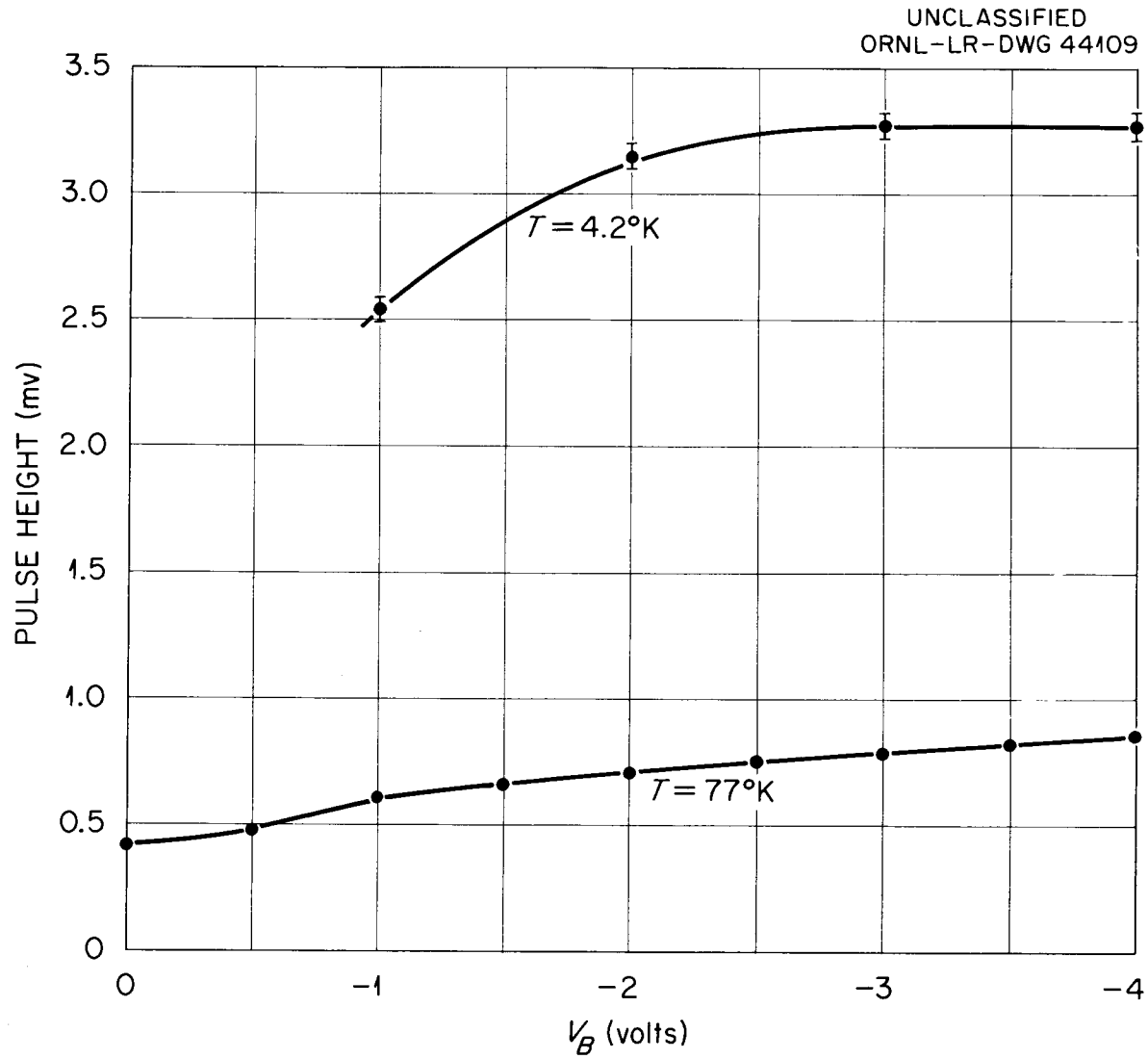

Figure 11. Counter pulse height as a function of applied bias voltage.

amperes flowing) had negligible effect at 77°K, 4.2°K, and 0.2°K. At 4.2°K and below, a field of 5000 gauss (the field of the refrigerator magnet) rendered the counter inoperative. All counting data were therefore taken with the refrigerator magnet turned off.

Thermometers. An accurate knowledge of the sample temperature was essential. The basic temperature standards used were helium vapor pressure ($1.2^{\circ}K < T < 4.2^{\circ}K$) and magnetic susceptibility of the paramagnetic salt ($T < 1.2^{\circ}K$). However, these measured only the equilibrium temperature of the entire experiment and refrigerator assembly. In addition, a resistance thermometer was installed within the sample capsule. A radio resistor[34] with the insulation ground off was glued into a copper block roughly approximating the size and shape of the sample. This was then mounted so that there was a high thermal resistance between the copper block and the other parts of the experiment. The thermometer was therefore cooled only by the helium-3 gas. The measured temperature rise, when the input power was increased from a negligible amount to the calculated alpha-particle heating of the sample, was an estimate of the temperature difference between the sample and the rest of the experiment. The resistance thermometer had, of course, to be properly calibrated against the basic temperature standards mentioned above.

Sample. The heating due to the high alpha activity made it impractical to use a single crystal of neptunyl rubidium nitrate. A

---

[34] Allen-Bradley Co., Milwaukee, Wisconsin, Type AB-$\frac{1}{2}$.

sample weighing 1.4 grams (the weight of the base crystal actually used) would be a heat source of 10^4 ergs per minute, and would be difficult to cool to sufficiently low temperatures. A thin layer of neptunyl rubidium nitrate was therefore grown onto a base crystal of the isomorphous compound uranyl rubidium nitrate, whose alpha-particle heating is 2000 times smaller.

In earlier work, x-ray diffraction studies by R. D. Ellison[35] have confirmed that the base (uranyl) crystals are indeed single crystals, and that the neptunyl "coating" grows in the same lattice, oriented in the same direction. A small chip fractured from such a sample was studied using Laue reflections from several points on the "outside" (neptunyl) and "inside" (uranyl) exposed surfaces. All showed the same structure and orientation. This was confirmed using "precession" diffraction photographs. The x-ray studies were made after the sample had been cycled repeatedly to low temperatures. For samples several months old, no evidence was found of thermal or radiation damage leading to disorientation of the crystal. Some samples a year old or more have a milky appearance, with a light-colored matte surface, and may be disoriented to some degree.

The sample crystals were grown from a saturated solution of uranyl rubidium nitrate in 16 M. nitric acid at approximately 50°C. The base crystals were seeded mechanically on the tips of platinum wires, which were then rotated slowly in the solution. For coating with the neptunium

---

[35] R. D. Ellison, Oak Ridge, Tennessee, private communication.

salt the dry, warm crystal was dipped briefly in warm 16 M. nitric acid, then immediately placed in a warm saturated solution of neptunyl rubidium nitrate and rotated slowly for the required time. The neptunyl salt coating rate was approximately 1 mg per minute.

The crystal which was used in this experiment had large cap faces and small prism faces. It showed essentially perfect form, with few visible imperfections. There was one crack about one-third through the center, which did not impair the usefulness of the sample. The crystal showed no evidence of any sort of damage (radiation or otherwise) when it was examined after the conclusion of the experiment. A sample from the base crystal of uranyl salt was checked in an alpha-particle energy analyzer, and was found to consist of uranium-234, -235, and -238 as expected in normal uranium. The total alpha-particle heating of the base crystal was calculated to be 6.1 erg/min.

When thin coatings are grown on such a crystal, it is difficult to determine the amount of salt in the coating layer by weighing, since an etching process precedes the coating. Therefore, the crystal was covered with thin aluminum foil, and the alpha particles emitted through a hole of known area by a typical cap face and a typical prism face were counted. From these data and the measured surface area of the crystal the total quantity of neptunium-237 present was inferred. In this way it was determined that there was 2.0 mg of neptunyl salt, whose alpha-particle heating was calculated to be 5.7 erg/min. The coating thickness was 0.75 mg/cm^2, an appreciable fraction of the alpha-particle range in

this material, which is estimated to be 5 mg/cm^2.[36]

The betas emitted by the sample were studied with a scintillation counter and absorbers, and the sample gamma radiation was analyzed using a scintillation spectrometer. The energies and intensities of the observed radiations were consistent with the amounts of uranium and neptunium known to be present, and their radioactive decay products. There was no evidence of any radioactive contamination.

Only one sample was used in this experiment. The earlier work has made it clear that such data are reproducible from sample to sample.

II. EXPERIMENT AND REFRIGERATOR ASSEMBLY

The low temperatures required for this experiment were attained by using adabatic demagnetization of a paramagnetic salt.[37] Manganous ammonium sulfate hexahydrate crystals (187 gm) were tamped into a brass cylinder 14.4 cm long and 4.0 cm in diameter, around and between five copper fins ($1\frac{1}{2}$ mm thick) which were silver-soldered to the experiment capsule (see Figure 7, page 28). The salt crystals had diameters ranging roughly from 0.1 to 1.5 mm. The interstices between the salt particles were then filled with toluene to increase heat transfer to the fins. The assembly of experiment capsule and paramagnetic salt was suspended

---

[36] H. A. Bethe and J. Ashkin, in E. Segre (ed.), Experimental Nuclear Physics (John Wiley and Sons, Inc., New York, 1953), I, 222.

[37] D. DeKlerk and M. J. Steenland, in C. J. Gorter (ed.), Progress in Low Temperature Physics (North-Holland Publishing Co., Amsterdam, 1955), I, 273.

by cotton threads in a space which could be pumped to a fairly high vacuum. The pressure measured at the room-temperature end of the pumping line was about 2×10^{-6} mm Hg whenever the experiment temperature was below $1^{\circ}K$. It should be noted that helium adsorption and condensation on the outside surface of the demagnetized assembly would reduce the pressure in the exchange gas space to a very low value. This was confirmed by the long warmup times (> 10 hours) which were observed.

Eight electrical connections had to be made to the experiment capsule. In order that these should not constitute a serious heat leak, they were made of constantan alloy wire, 0.005 cm in diameter and about 1 meter long. The wires were coated with a very thin layer of tin-lead solder, which would be superconducting at temperatures below about $7^{\circ}K$. They were then wound into solenoidal coils 3 mm in diameter, which were stretched axially so that adjacent turns did not touch. The wires thus had essentially zero electrical resistance, but conducted heat very poorly, as required.

When it was desired to bring the experiment and refrigerator assembly into good thermal contact with the liquid helium bath, helium-4 gas could be admitted into the vacuum space, as shown in Figure 6, page 27. This exchange gas was used during calibration of the susceptibility coils and the resistance thermometer in the temperature range $1.2\text{-}4.2^{\circ}K$. On the other hand, for the adiabatic demagnetizations, thermal contact was made--and disconnected--by means of a "heat switch" based on the work

of Webb and Wilks,[38] and of Berman.[39] A pair of jaws operated by a pullrod could be opened, or closed to pinch a copper post which was part of the experiment capsule. The jaw tips were connected thermally to the liquid helium bath. The post and jaws were gold plated to increase the thermal conductivity of the junction. By using the heat switch, it was possible to proceed with the entire demagnetization process without using exchange gas; this resulted in a reduction in the time required, and, more important, in the residual exchange gas heat leak.

III. DEWARS AND REFRIGERATOR MAGNET

The experiment was contained in a double dewar vessel, with liquid nitrogen in the outer space and liquid helium in the inner space. The liquid helium space was connected via a large pipe to a Kinney mechanical pump whose capacity was 40 standard liters per second. Suitable manometers filled with mercury and with dibutyl phthalate were installed to read the helium bath vapor pressure. The temperature of the liquid helium could be reduced to $1.14^{\circ}K$; the loss rate varied between 80 and 120 cm^3 per hour.

A large electromagnet was used to produce the magnetic field employed in the adiabatic demagnetization process. Current to the magnet

---

[38] F. J. Webb and J. Wilks, Proc. Roy. Soc. (London) A230, 549 (1955).

[39] R. Berman, J. Appl. Phys. 27, 318 (1956).

was supplied by a motor-generator set, excited by an amplidyne generator, which was manually controlled. Only 5000 gauss was needed to attain $0.2^{\circ}K$; this was easily produced at a current of 40 amperes. The magnet could be rolled on rails to get it out of the way when it was not in use.

IV. SAMPLE ROTATION

The magnetic field for rotating the sample was produced by a pair of vertical Helmholtz coils which could be brought into positions on opposite sides of the dewar vessels, and which could then be rotated mechanically about an axis which coincided approximately with the axis of rotation of the sample. The angular position of the Helmholtz coils could be set and read to $\pm 0.1^{\circ}$. This magnetic field produced a torque on the permanent magnet attached to the sample holder. (The assembly was made so that the large field of the refrigerator magnet would align the sample at about $\theta = 45^{\circ}$.) Current for the Helmholtz coils was obtained from a bank of large storage batteries, and was regulated manually using rheostats.

The basic measurement of sample rotation angle was made using the condenser plates. These were set up--in their bearings--in a dividing-head goniometer and the function $C(\theta)$ determined. The measurement of this capacitance in the experiment was complicated by the extra capacitance of the long leads involved ($\approx$ 150 pf) and by the fact that the capacitance measurement upset the counter and perhaps the thermometer as well. For this reason, it was not possible to use capacitance measurements to determine rotation angles while counting. Accordingly, the

relationship between the sample rotation angle and the Helmholtz coil angle was determined once, using the condenser, as a function of the current in the Helmholtz coils. At a current of 20 amperes, the angular error was no more than $\pm 1^{\circ}$. All angular distributions were therefore done at 20 amperes.

The situation was different for counting at $\theta = 0^{\circ}$ and $\theta = 90^{\circ}$. As was previously mentioned, there were electrically insulated stops at these angles, and a simple check of electrical continuity through the stops to the grounded sample holder confirmed that the sample was actually at these positions. For counts at these angles, the Helmholtz coils were rotated past the desired point by an appropriate amount ($3\text{-}5^{\circ}$ at 20 amperes, 30° at 5 amperes) and the position was confirmed with a continuity check.

V. INSTRUMENTATION

A block diagram of the instrumentation is shown in Figure 12. The pulses were amplified in a special low-noise preamplifier designed by E. Fairstein,[40] the output of which was connected to an A-1D linear amplifier.[41] The pulse height selector in the amplifier produced an output pulse each time the amplified input pulse exceeded the preset discrimination level. In order to study the variation (if any) of the anisotropy

---

[40] E. Fairstein, Oak Ridge, Tennessee, private communication.

[41] P. R. Bell and C. C. Harris, Oak Ridge, Tennessee, private communication.

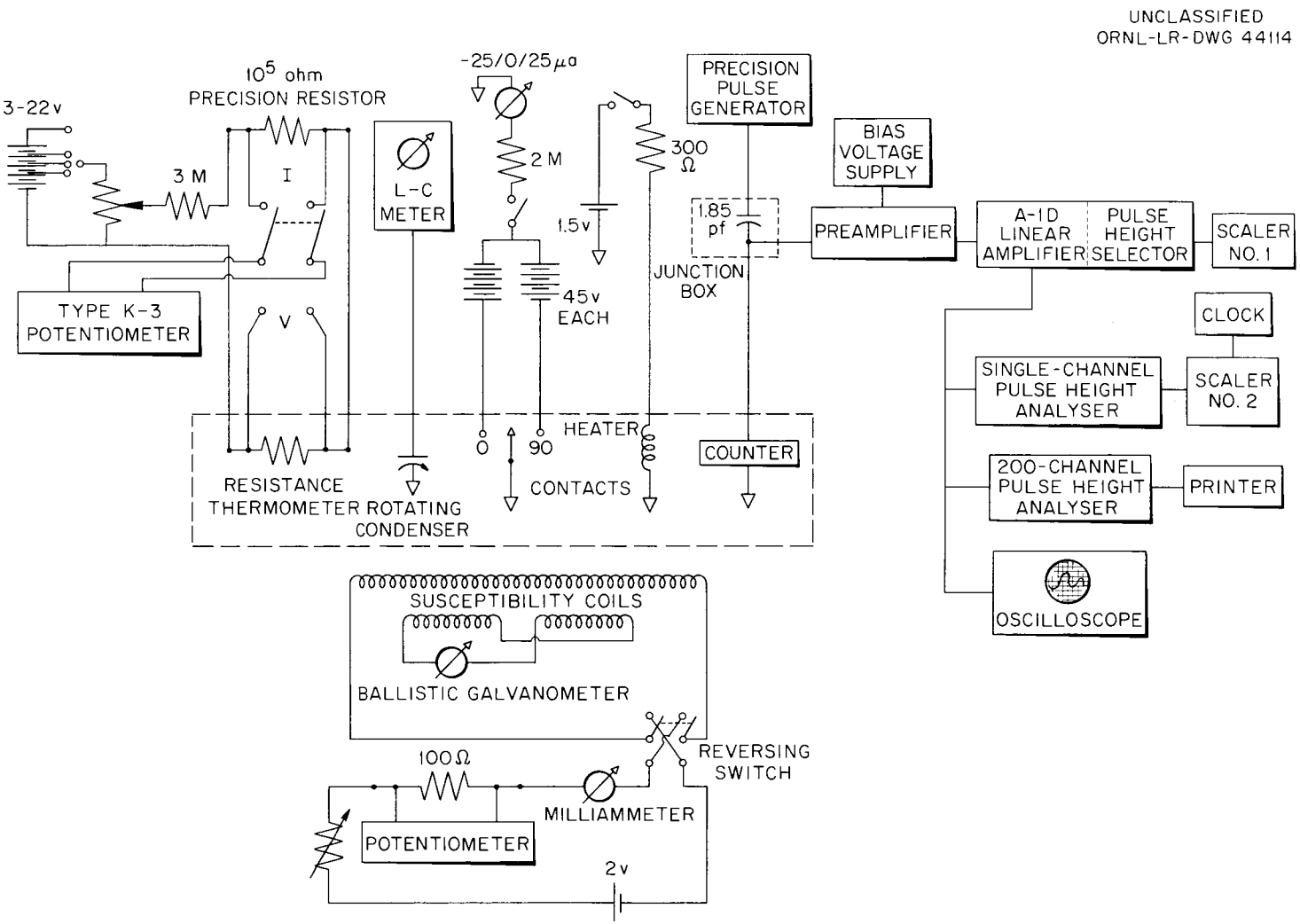

Figure 12. Block diagram of instrumentation.

with discrimination level, an additional pulse height selector[42] was used, and both sets of output pulses were counted. Bias voltage for the counter was supplied by a simple dry cell-voltage divider arrangement. The pulse height distribution curves of runs 25, 26, and 27 were obtained using a 200-channel pulse height analyser.[43]

The voltage across and the current through the resistance thermometer were measured using a Type K3 Potentiometer.[44] The current supply for the measurement was a dry cell and voltage divider, with suitable series resistors for current measurement and current limiting.

The magnetic susceptibility of the paramagnetic cooling salt was measured by detecting changes in the mutual inductance of coils wound around the salt volume. An identical mutual inductance was connected in opposition. The measurement was made using a ballistic galvanometer. The primary current was measured to $\pm$ 1 part in 10^4 with a portable potentiometer.

The capacitance of the condenser plates was measured with an "L C meter"[45] which places the unknown reactance in an oscillator resonant circuit and measures the frequency with a heterodyne detector. The capacitance could be read to $\pm \frac{1}{2}$ pf.

---

[42] J. E. Francis, Jr., P. R. Bell, and J. C. Gundlach, Rev. Sci. Instr. 22, 133 (1951).

[43] Radiation Instrument Development Laboratory, Inc., Chicago, Illinois, Model 34-9.

[44] Leeds and Northrup Company, North Wales, Pennsylvania, Model 7553.

[45] Tektronix, Inc., Portland, Oregon, Type 130.

CHAPTER V

EXPERIMENTAL PROCEDURE AND RESULTS

I. COUNTING

All counting was done either with two pulse height selectors set at different discrimination levels, or with the multichannel analyser and one pulse height selector. The data for runs 2-14 consisted of series of counts at $\theta = 0^\circ, 90^\circ, 90^\circ, 0^\circ$ in that order so that any possible slow drifts would be cancelled. In order to minimize friction heating in the bearings, these rotations were performed by turning off the current to the Helmholtz coils, rotating them to the new position, and slowly increasing the current until the electrical contact indicator showed that rotation was complete. The current in the Helmholtz coils was left on during the counting.

For the angular distributions of runs 15-25, the current in the Helmholtz coils was maintained at 20 ± 0.5 amperes at all times; the coils were rotated slowly with the current on. The counting sequence was $\theta = 0^\circ, 15^\circ, 30^\circ, ---, 75^\circ, 90^\circ, 90^\circ, 75^\circ, ---, 0^\circ$. In this way at least two separate counts were taken at each angle for each run, again in such a way as to cancel any slow drift.

II. TEMPERATURE MEASUREMENT

Vapor pressure. Whenever helium-4 exchange gas coupled the sample capsule thermally to the liquid helium bath, the temperature was best determined by measuring the vapor pressure over the helium bath and

correcting, at temperatures above the λ point, for the weight of the liquid helium above the sample. The vapor pressure-temperature scale used was T55E, as compiled by Clement.[46] The manometer height could be read to ± 0.05 mm; this gives an accuracy of ± 0.001°K or better.

Magnetic susceptibility. At temperatures below 1.14°K, the temperature was determined by measuring the magnetic susceptibility of the paramagnetic salt. This method was also used whenever the temperature was above 1.14°K, without exchange gas present. The magnetic thermometer was carefully calibrated against helium vapor pressure at several points between 1.14°K and 4.2°K, with exchange gas present. The calibration curve is shown in Figure 13.

The corrections which must be made to susceptibility data are discussed by Casimir[47] and by Kurti and Simon.[48] The "local" magnetic field at the atom is given by

$$H_L = H_0 + \frac{4\pi}{3}\frac{M}{V} - \left(\alpha_e + \frac{4\pi}{3}\frac{1-f}{f}\right)\frac{M}{V} \tag{23}$$

H_L = Local magnetic field

H_0 = Applied magnetic field

M = Magnetization

---

[46] J. R. Clement, J. K. Logan, and J. Gaffney, Phys. Rev. 100, 743 (1955), see note added in proof.

[47] H. B. G. Casimir, Magnetism and Very Low Temperatures (University Press, Cambridge, England, 1940), pp. 9-13.

[48] N. Kurti and F. Simon, Phil. Mag. 26, 849 (1938).

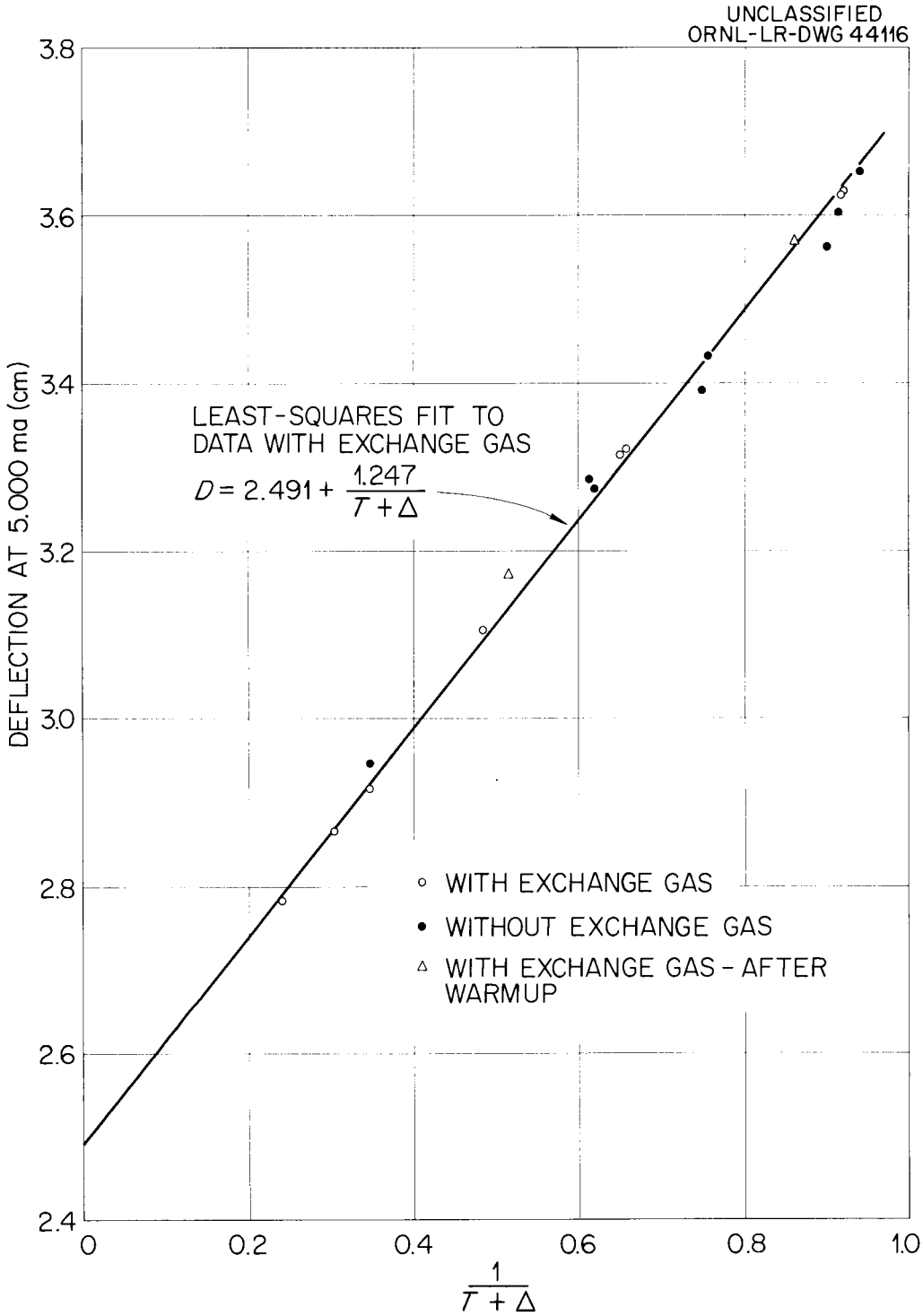

Figure 13. Susceptibility calibration.

V = Volume

α_e = Ellipsoid demagnetization factor

f = Powder filling fraction.

This equation is valid only for ellipsoidal-shaped salt samples with H_0 along one of the principal axes, since only for this case will H_0 and H_L be in the same direction. The thin slabs of salt were approximated by ellipsoids of the same aspect ratios ($b/a = 0.516$, $c/a = 0.0297$); the demagnetizing factor given by Osborn[49] is $\alpha_e = 0.201$. The powder fraction was determined from the measured weight of salt used, the available volume, and the crystalline density[50] of 1.83. The result is $f = 0.683$. Susceptibility data are conventionally corrected to the susceptibility which would be measured if the salt were a solid sphere at the same temperature. For this case, $H_L = H_0$, since $\alpha_e = \frac{4\pi}{3}$ and $f = 1.0$. The magnetic temperature $T^{\circledast}$ is then defined by

$$T^{\circledast} = \frac{C}{\chi\ \text{sphere}} = \frac{C}{\chi\ \text{meas}} - C\left\{f\left[\alpha_e + \frac{4\pi}{3}\,\frac{1-f}{f}\right] - \frac{4\pi}{3}\right\}$$

$$= \frac{C}{\chi\ \text{meas}} + 0.056^{\circ}\text{K} = \frac{C}{\chi\ \text{meas}} + \Delta, \qquad (24)$$

where χ_{meas} is the apparent susceptibility as measured and Δ is a calculated correction. Finally, there is a constant multiplier to relate galvanometer deflection to susceptibility and a subtraction for

---

[49] J. A. Osborn, Phys. Rev. 67, 351 (1945).

[50] J. W. Mellor, Comprehensive Treatise on Inorganic and Theoretical Chemistry (Longmans, Green and Co., London, 1932 and 1942), XII, 415.

residual mutual inductance when $\chi = 0$. A least-squares fit to all calibration points gives

$$T^{\circledast} - 0.056 = \frac{1.247}{D_5 - 2.491}, \tag{25}$$

where D_5 is the measured deflection in cm at a primary current of 5.000 mA.

A measured relationship between $T^{\circledast}$ and the thermodynamic temperature T is given by Cooke, Meyer, and Wolf;[51] these data were used to determine T from magnetic measurements.

Resistance thermometer. Measurements were made with the resistance thermometer for each run where the temperature was below 1.2°K. At temperatures below 0.5°K, the temperature of the resistance thermometer increased measurably above its surroundings when its electrical heat input was set to 0.02 microwatts, which was the calculated sample alpha-particle heating rate. These data are plotted as a function of temperature in Figure 14, for all runs except Run 27. Electrical breakdown invalidated this measurement for Run 27. The smoothed curve of Figure 14 was used to estimate an upper limit for the sample temperature for each run.

Heat transfer in helium-3 gas. The temperature rise of the sample above its surroundings may also be estimated by calculating the heat transfer of the helium-3 gas. At a temperature of 0.2°K, DeBoer[52]

---

[51] A. H. Cooke, H. Meyer, and W. P. Wolf, Proc. Roy. Soc. (London) A233, 536 (1956).

[52] J. DeBoer, in C. J. Gorter (ed.), Progress in Low Temperature Physics (North-Holland Publishing Company, Amsterdam, 1955), I, 401.

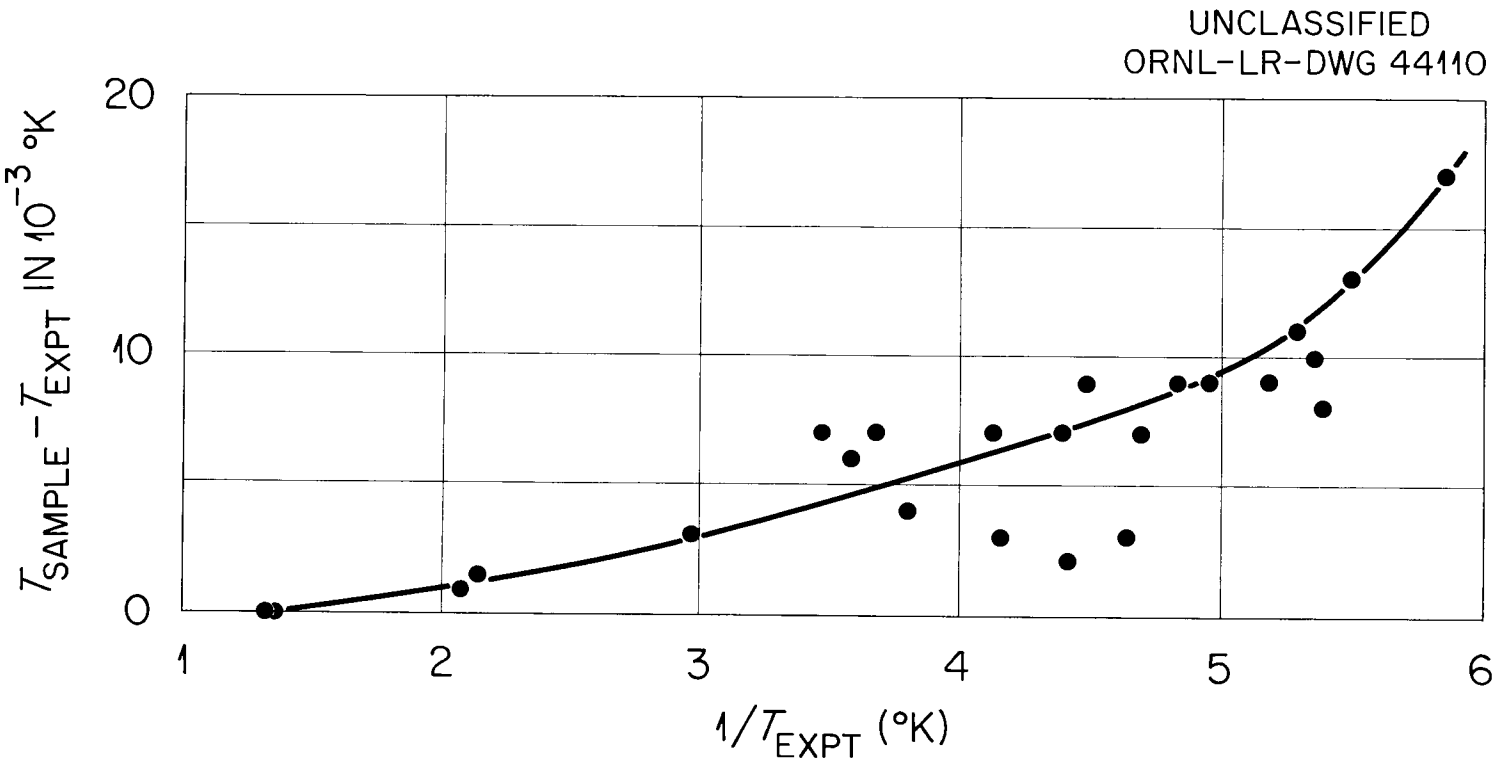

Figure 14. Temperature rise of the resistance thermometer at a power input of 0.02 microwatt.

gives the coefficient of heat conduction as 200 erg/sec cm ^{o}K. A spherical sample with a heating rate of Q = 0.02 μwatt and a radius of 0.46 cm will be only 2×10^{-4} ^{o}K above its surroundings at this temperature. This calculation assumes that the mean free path of a helium molecule is short compared to the dimensions of the system. A classical estimate of the mean free path at 0.2^{o}K is roughly 1 cm;[53, 54] quantum effects will decrease this.

The measured temperature rise of the resistance thermometer at Q = 0.02 μwatt was at least an order of magnitude greater than the temperature rise calculated on the basis of helium-3 thermal conductivity.

Clement and Quinnell[55] give an empirical relationship for the temperature rise of 1-watt Allen-Bradley resistors in the temperature range 1-4°K:

$$dQ/dT = 2.5 \times 10^{-4}\ T \text{ watt/degree.} \tag{26}$$

If one assumes that this relation holds at T = 0.2^{o}K, then for Q = 2×10^{-8} watt, the result is $\Delta T = 10^{-4}$ ^{o}K at this temperature. The thermal conductivity of the G. E. 7031 cement and of the carbon resistor itself might be expected[56] to decrease markedly when the temperature was

---

[53] R. D. Present, Kinetic Theory of Gases (McGraw-Hill Book Co., Inc., New York, 1958), p. 32.

[54] Charles D. Hodgman (ed.), Handbook of Chemistry and Physics (Chemical Rubber Publishing Co., Cleveland, Ohio, 1958), 40th ed., p. 3373.

[55] J. R. Clement and E. H. Quinnell, Rev. Sci. Instr. 23, 213 (1952).

[56] J. C. Wheatley, D. F. Griffing, and T. L. Estle, Rev. Sci. Instr. 27, 1070 (1956).

reduced to $0.2^{\circ}K$. The measured temperature rise at low temperatures was therefore presumably due to reduced thermal conductivity of the resistance thermometer, and gave only an upper limit to the sample temperature rise.

III. PULSE HEIGHT ANALYSIS

In Figure 15 are shown typical pulse height distributions under various conditions. The data were obtained using a 200-channel pulse height analyser. The variation of counting rate with channel number is the differential pulse height distribution; the total number of counts is the sum of the counts in all the channels. Conventionally, the summation is done only over channels above a certain voltage, denoted the discrimination level. This is done because pulses of low height may be due to noise in the counting system. The variation of this sum (the integral counting rate) with discrimination level is the integral pulse height distribution. The pulse height selectors in the A-1D amplifier and the single-channel analyser (see Figure 11) give one output pulse each time an incoming pulse exceeds a preset discrimination level; the counting rate from these instruments is therefore just the integral counting rate defined above.

At $77^{\circ}K$, counters of the type used in this experiment are known[57] to count alpha particles with a resolution of about 200 Kev, and with a peak pulse height proportional to the alpha-particle energy. The $77^{\circ}K$

---

[57] Walter, Dabbs, and Roberts, loc. cit.

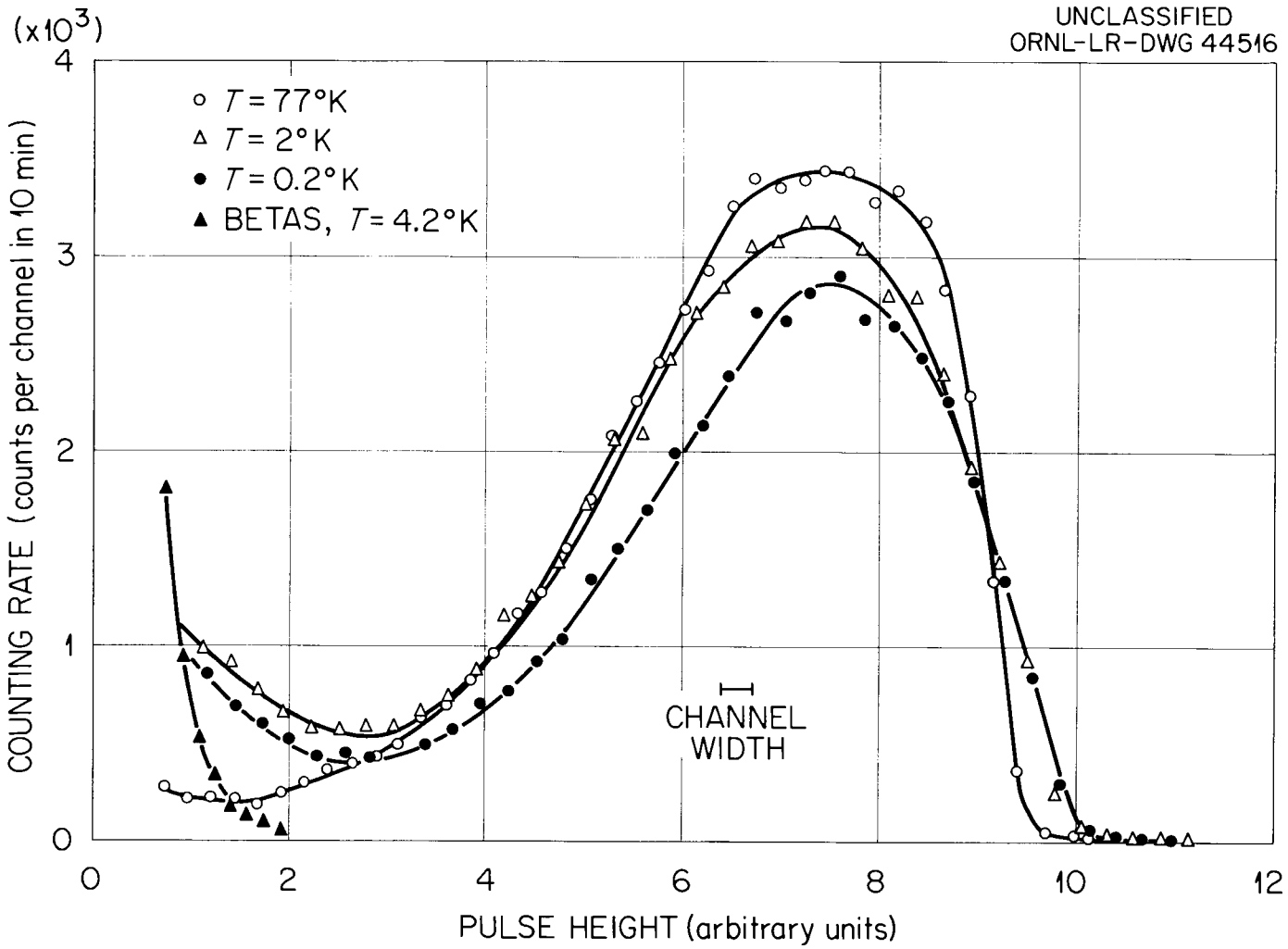

Figure 15. Typical pulse height distributions at $\theta = 0^{\circ}$.

pulse height distribution shown in Figure 15 is therefore presumably representative of the spectrum of alpha particles emerging from the sample. Alpha energy analysis of the same sample in a gridded ionization chamber gave a pulse height distribution in satisfactory agreement with the shape of the 77°K pulse height distribution shown in Figure 15.

The pulse-height distributions at 2°K and at 0.2°K shown in Figure 15 show that the shape of the distribution was substantially changed at low temperature. The resolution was poorer--as evidenced by the decrease of the slope at the high-energy end of the distribution--and there was a group of small pulses which did not appear at 77°K. The increase in resolution width has been observed previously by Walter.[58]

Beta rays. The small pulses were hypothesized to be due to beta rays, whose range in germanium is comparable to the thickness of the counter, and which could therefore be counted with good efficiency when the bulk resistivity of the germanium was high, but which would produce negligibly small pulses when the counter temperature was 77°K. A source of 2.3 Mev beta rays existed in the material of the base crystal, in the beta decay of the isomeric state of protoactinium-234.

A beta experiment was performed by admitting sufficient helium-4 gas into the experiment capsule to stop all the alpha particles before they could reach the counter. This "gas shutter," whose thickness was 5 mg/cm^2, had a negligible effect upon the 2.3 Mev betas, whose range is

---

[58] F. J. Walter, Oak Ridge, Tennessee, private communication.

about 1 gm/cm^2. The results of this experiment are shown in Figures 16 and 17. The betas were isotropic, and the integral counting rate was an exponential function of the discriminator setting, as would be expected for a thick source. The beta pulse height distribution is compared with the observed alpha pulse height distributions in Figure 15. It is evident that the extra small pulses observed at 4°K and at 0.2°K were not due to beta rays. At the discrimination levels used, the beta counts were merely an isotropic "background" of altogether negligible effect. They were ignored in all further work.

Extra pulses. Portions of integral pulse height distributions are shown in Figure 18, for $\theta = 0^\circ$ and 90°, at T = 77°K and 2°K. Taking the 77°K data as the true counting rates, the counting rates at T = 2°K should have been decreased by about 4 per cent at $\theta = 0^\circ$, and increased by 2 per cent at $\theta = 90^\circ$, due to the effect of the nuclear alignment. The curves in Figure 18 show that this was so, very approximately, at high discrimination levels. However, as smaller pulses were added to the integrals, the counts at 2°K increased markedly relative to the counts at 77°K. At low discrimination levels, the small pulses increased the counts at 2°K to about 1.1 times the amount expected on the basis of the counts at 77°K.

The extra pulses appear to have had their origin in some mechanism in the germanium counter, since they did not appear in the data taken at 77°K, when everything but the sample and counter temperatures was the same as for the low-temperature data.

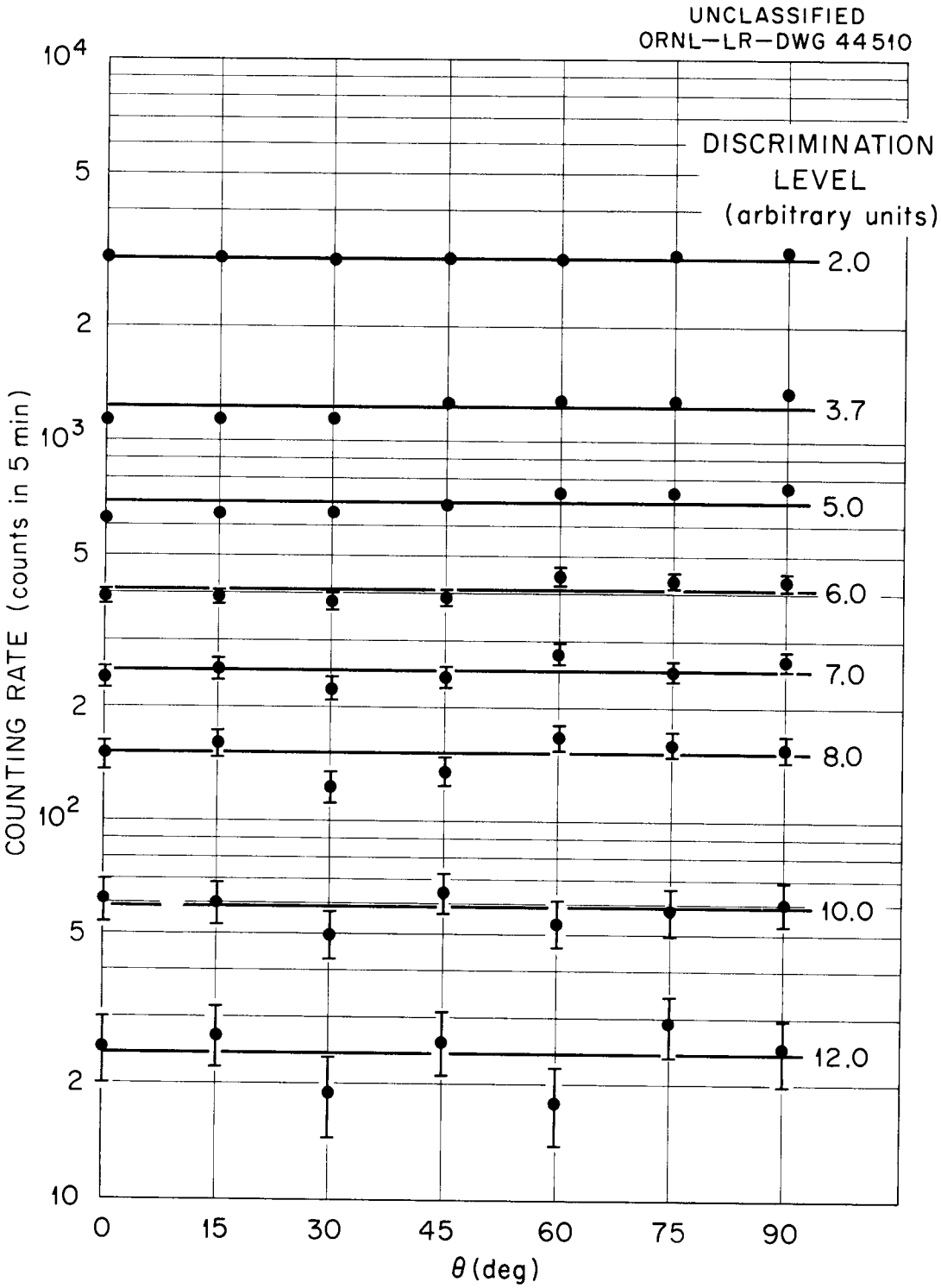

Figure 16. Beta integral counting rate as a function of angle and discrimination level.

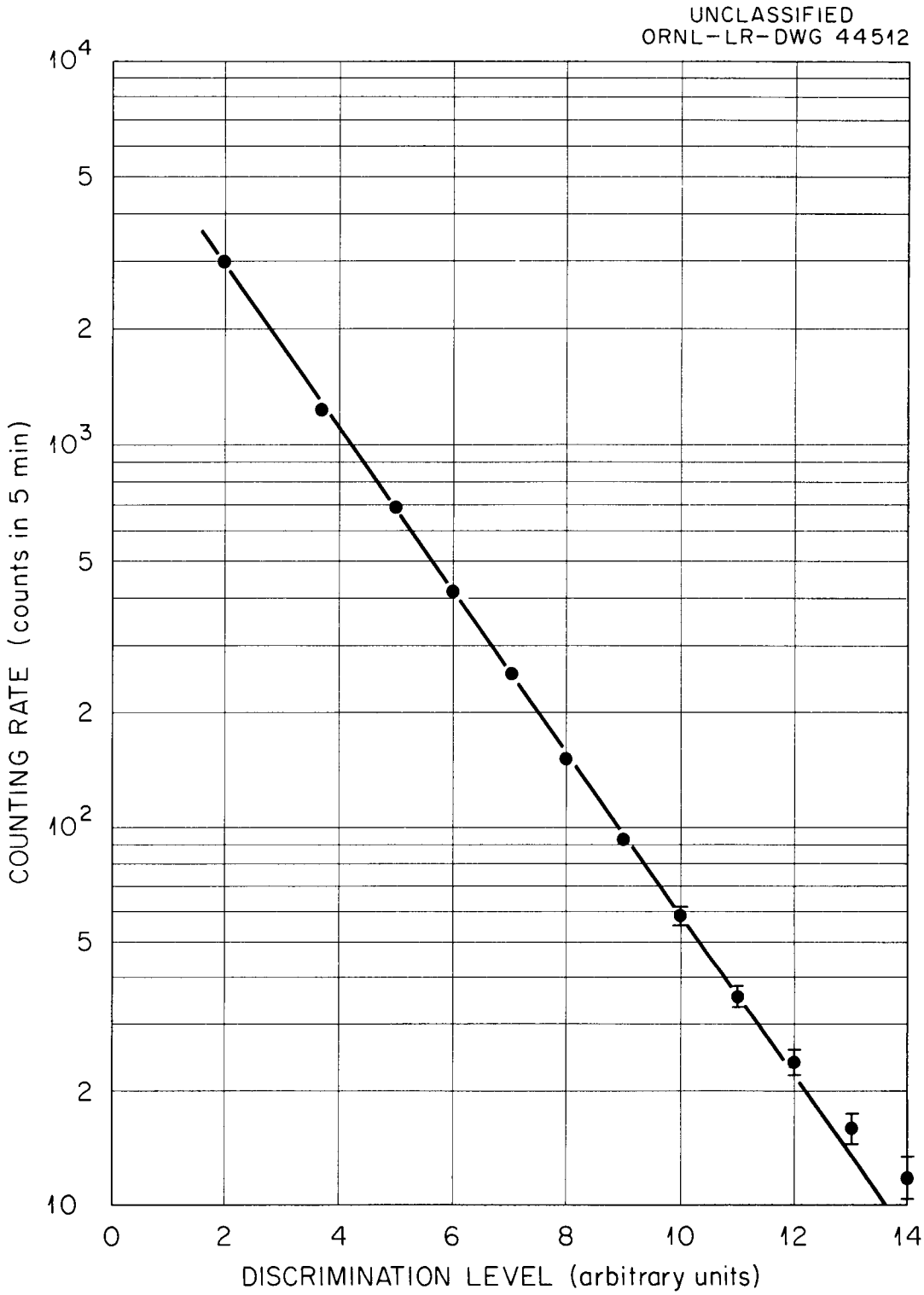

Figure 17. Beta integral counting rate (average over θ) as a function of discrimination level.

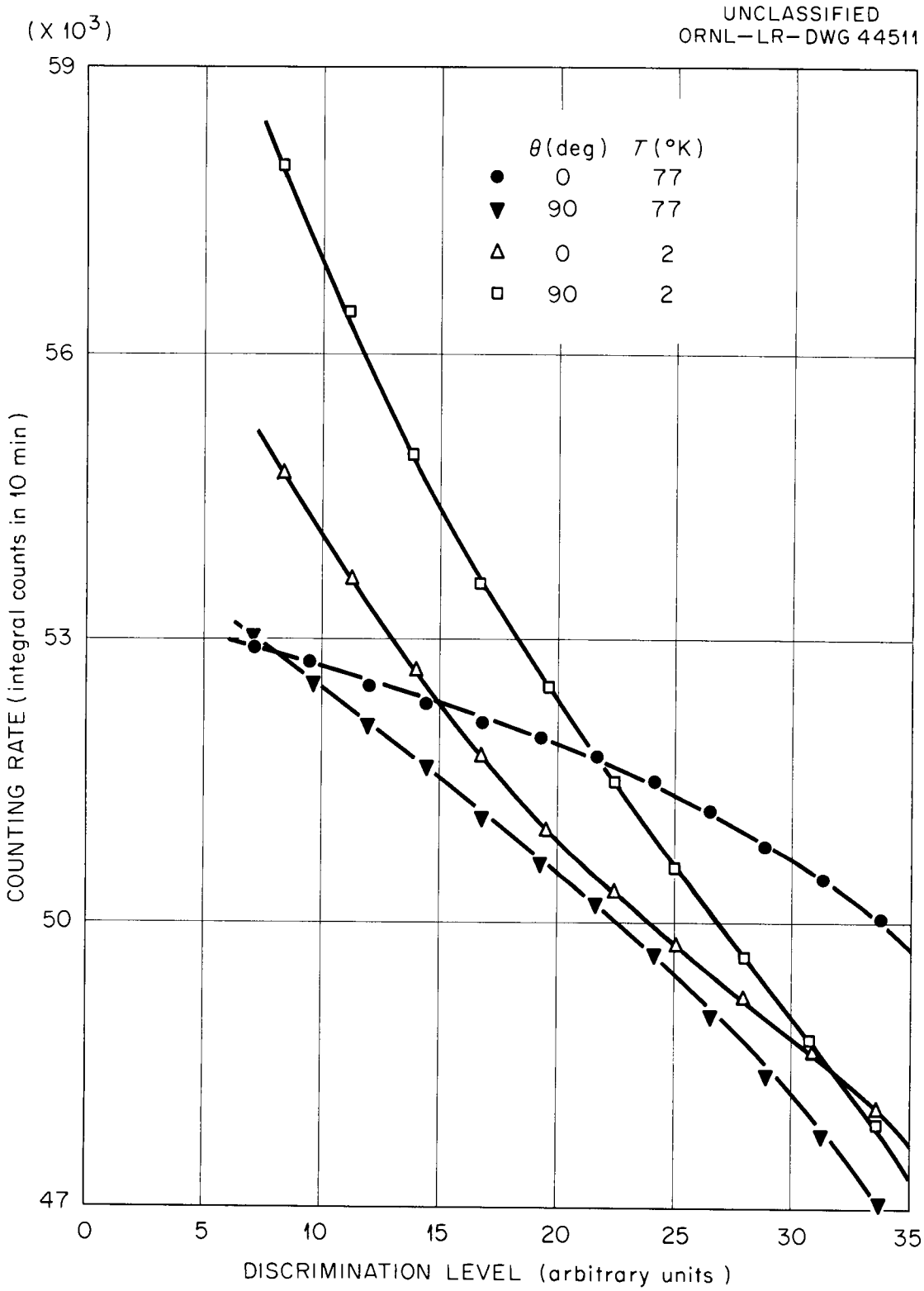

Figure 18. Integral pulse height distributions.

In spite of the fact that the "extra" pulses are of undetermined origin their number was shown to be proportional to the number of "real" alpha counts, by considering the ratio of the integral counting rate at $0.2^{\circ}K$ to the integral counting rate at $2^{\circ}K$. At each angle, this ratio was substantially independent of the discrimination level. The integral counting rate at low temperatures could therefore be taken as a measure of the true alpha emission rate, albeit with a scale factor, independent of θ or T, whose value of about 1.1 had to be determined experimentally.

IV. ANALYSIS OF ANGULAR DISTRIBUTIONS

The observed angular distribution is expected to have the form (neglecting P_4):

$$W'(\theta) = V(\theta,D)\left[1 + b_2F(T)P_2(\cos\theta)\right] \tag{27}$$

where

$V(\theta,D)$ = angular and integral pulse height distribution of alpha particles at high temperature

D = discrimination level

b_2 = correction for finite source and counter

F(T) = experimentally determined anisotropy coefficient, which is expected to be proportional to $G_2(T)$.

If the counter characteristics were the same at all temperatures of interest, $V(\theta,D)$ would be given directly by the data at $77^{\circ}K$, since F(T) is negligible at this temperature. However, the change in resolution between $77^{\circ}K$ and low temperatures, and the appearance of the "extra"

pulses, make this only a crude approximation. The angular distributions for Runs 26 and 27, determined in this way, are shown in Figure 19, where the ratio

$$\frac{W' \text{ (low temperature)}}{W'(77^{\circ}K)} \tag{28}$$

is plotted against $P_2(\cos\theta)$. Although a correlation is present, the scatter of the points is much worse than would be expected on the basis of counting statistics alone.

Since $W'(77^{\circ}K)$ is not a good approximation for the value of $V(\theta,D)$ applicable to the low-temperature data, the quantity $V(\theta,D)$ must be inferred from the data taken at low temperatures. This was done using Runs 4, 5, 10, 11, 12, 13, 14, 18, and 21, all of which were performed at temperatures in the range 1-4°K, and all at the same two discrimination levels, $D_{1,2}$. From these data, estimates of $V(\theta,D_{1,2})$ were calculated using the equation

$$V(\theta,D_{1,2}) = \frac{W'(\theta,D_{1,2})}{1 + b_2F(T)P_2(\cos\theta)} \ . \tag{29}$$

For each of these runs, the size of the quantity $b_2F(T)$ was estimated from the curves of $a_2G_2(T)$, normalized to earlier data, given in Figure 4. The estimates of $V(\theta,D_{1,2})$ agreed with each other within the expected statistical variation. Their average at each angle, weighted according to the statistical variance of each estimate, was used for $V(\theta,D_{1,2})$. The values of $W'(\theta)/V(\theta)$ were then fitted by least squares to Equation (27). Some angular distributions calculated in this way are shown in Figures 20 and 21. As will be shown below, the scatter of the points is just

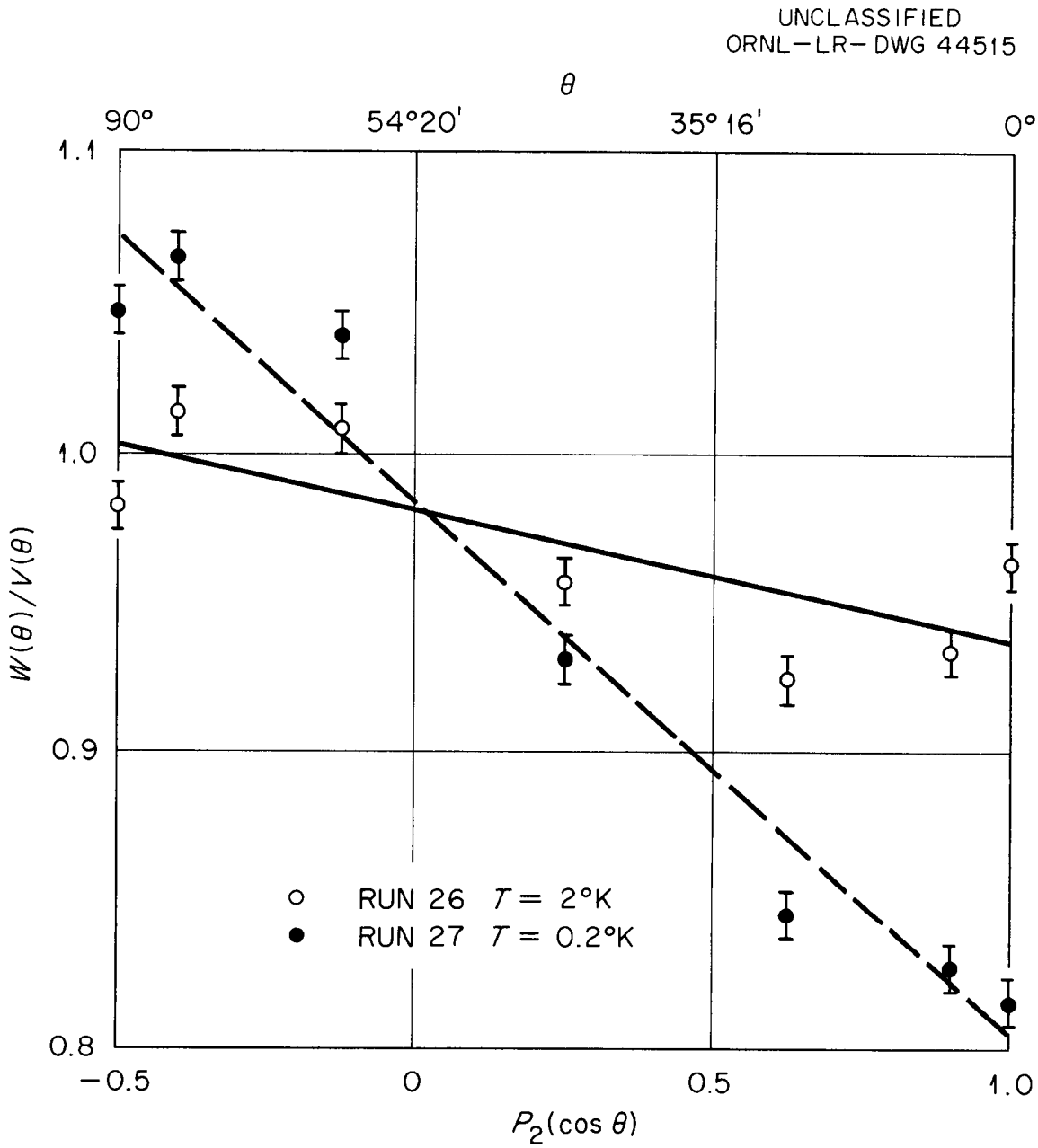

Figure 19. Angular distributions for Runs 26 and 27, using the data at 77°K for V(θ).

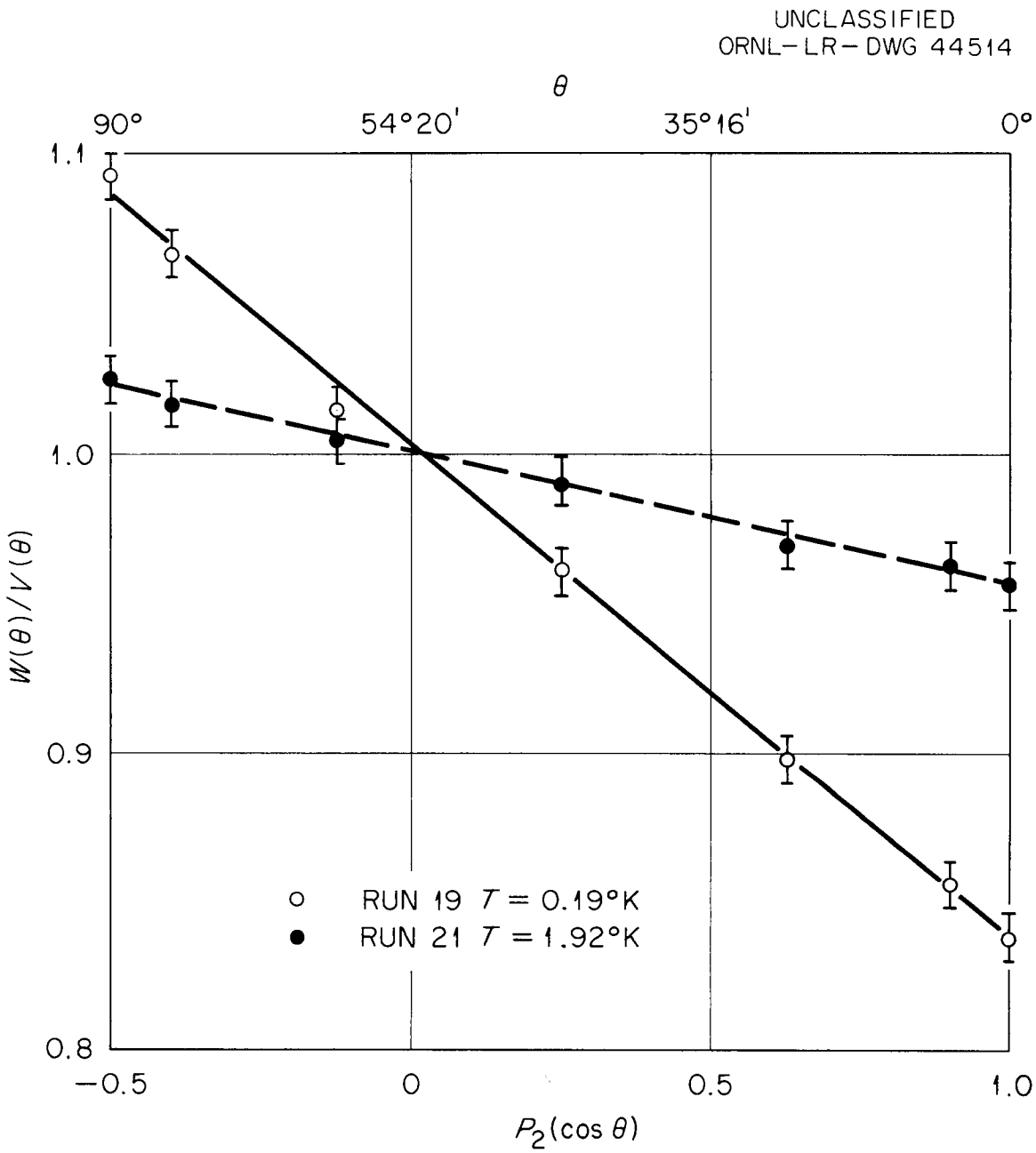

Figure 20. Angular distributions for Runs 19 and 21.

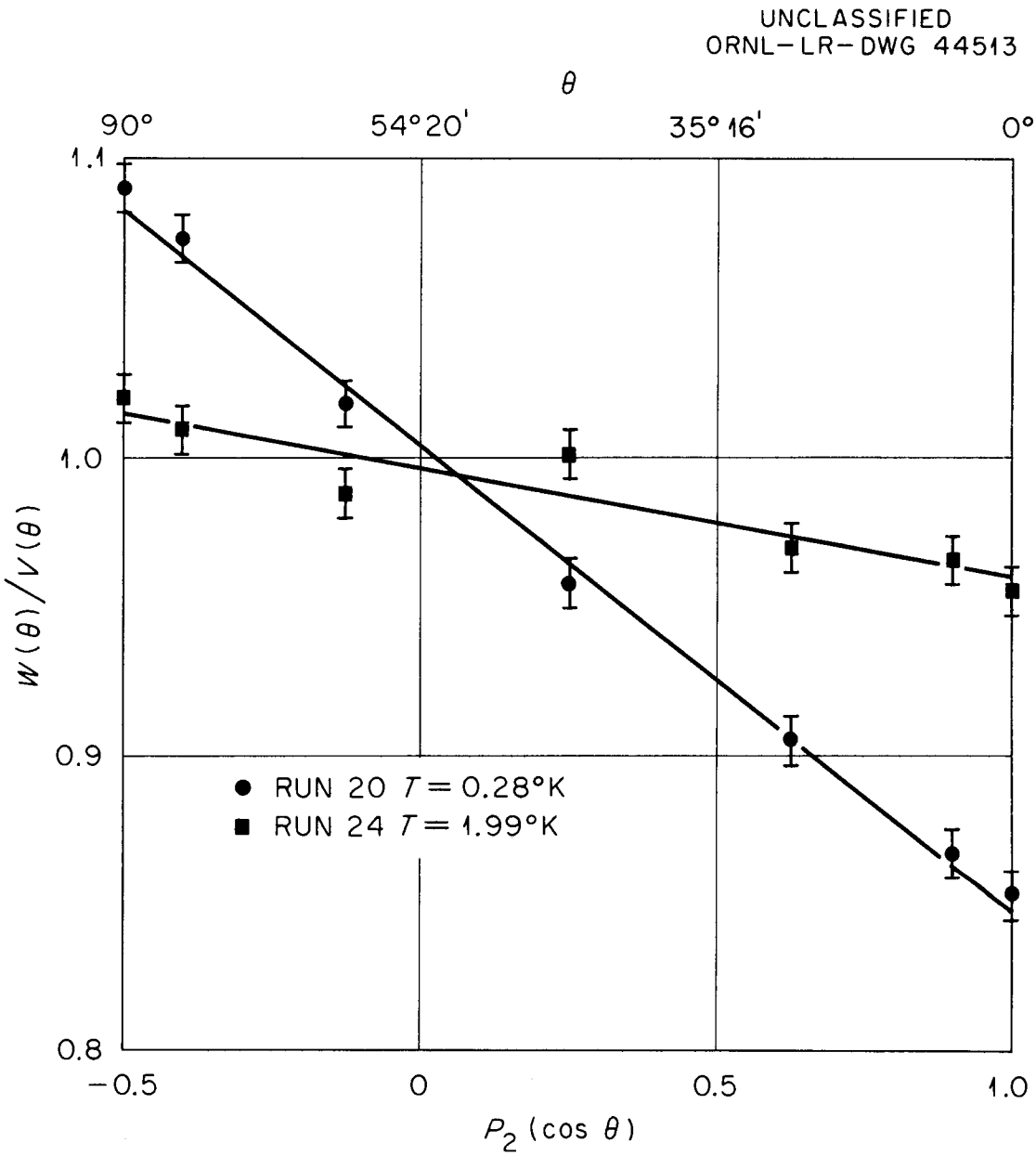

Figure 21. Angular distributions for Runs 20 and 24.

what might be expected from counting statistics.

Since Runs 24, 26, and 27 were performed with discrimination levels not equal to $D_{1,2}$, analyses using $V(\theta,D_{1,2})$ might be expected to show greater scatter of points around the best fit to $1 + b_2F_2P_2(\cos\theta)$, and they do (see Table II). For Run 24, the fit is adequate, since one of the discrimination levels used was very nearly equal to D_1. To determine whether an error could be introduced by improper choice of V, $V'(\theta,D_{26})$ was calculated from the data of Run 26 and the appropriate value of $b_2F(T)$. Runs 19, 20, 21, and 27 were then analysed using both $V(\theta,D_{1,2})$ and $V(\theta,D_{26})$. The least-squares values of $b_2F(T)$ obtained in the two ways are given in Table II. The values calculated for $b_2F(T)$ are evidently not sensitive to the choice of V or V'.

A summary of all results, including errors, is given in Table II. The values of $b_2F(T)$ determined for all the runs are shown as a function of temperatures in Figure 22, along with the two theoretical curves for $a_2G_2(T)$, normalized at $1.16^{\circ}K$. The data are clearly in agreement with the theoretical curve for the signs $A < 0$, $P > 0$, and the choice $A > 0$, $P < 0$ is excluded.

V. ERRORS

A statistical analysis was made of Runs 15-21, 24, 26, and 27 analysed with $V(\theta,D_{1,2})$ and Runs 19-21 and 27 analysed with $V'(\theta,D_{26})$. For each run, estimates of $\sigma(bF)$, the standard deviation of $b_2F(T)$, were made using the deviations of the individual counts from the least-squares best fit line. These were found to be in satisfactory agreement

TABLE II

SUMMARY OF RESULTS

Run Number	Number of Angles Counted	Sample Temperature T (°K)	$\frac{1}{T}$ (°K)$^{-1}$	$b_2F(T)$ [a]	$\sigma(bF)$ statistical [b]	$\sigma(bF)$ experimental (2 values) [c]		$\sigma(bF)$ averages [d]
1	2	77	0.013					
2	2	2.80	0.357	-.030	.0052			
3	2	2.96	0.338	-.024	.0052			
4	2	1.66	0.602	-.057	.0052			
5	2	1.17	0.855	-.062	.0052			
6	2	0.215	4.65	-.169	.0100			
7	2	0.235	4.26	-.155	.0052			
8	2	0.338	2.96	-.142	.0052			
9	2	0.760	1.32	-.097	.0052			
10	2	4.21	0.238	-.018	.0052			
11	2	2.95	0.339	-.021	.0052			
12	2	2.10	0.476	-.042	.0052			
13	2	1.57	0.637	-.052	.0052			
14	2	1.15	0.870	-.070	.0052			
15	7	0.226	4.42	-.149	.0054	.0050	.0106	
16	7	0.281	3.56	-.136	.0054	.0055	.0042	.0058
17	7	0.477	2.10	-.094	.0054	.0027	.0048	
18	7	1.14	0.877	-.064	.0054	.0045	.0091	
19	7	0.191	5.24	-.163	.0034	.0035	.0035	
20	7	0.281	3.56	-.154	.0034	.0036	.0044	
21	7	1.92	0.521	-.044	.0034	.0014	.0018	.0030
22	7	77	0.013					
23	7	77	0.013					
24	7	1.99	0.503	-.037	.0034	.0029		
25	7	77	0.013					
26	7	1.99	0.503	-.028	.0034	.0058		
27	7	0.196	5.10	-.163	.0034	.0044		
19[e]	7	0.191	5.24	-.165	.0034	.0040		
20[e]	7	0.281	3.56	-.155	.0034	.0045		
21[e]	7	1.92	0.521	-.043	.0034	.0048		
27[e]	7	0.196	5.10	-.163	.0034	.0057		

[a] From $W(\theta) = V(\theta,D)[1 + b_2F(T)P_2(\cos\theta)]$.

[b] Calculated on the basis of number of counts only.

[c] Two values given from the results at the two discrimination levels used ($D_{1,2}$), Runs 15-21.

[d] Averages over runs expected to have the same value of $\sigma(bF)$.

[e] These four values were computed using $V'(D_{26})$; for all others $V(D_{1,2})$ was used.

with the standard deviation inferred from the counting statistics. The results are tabulated in Table II.

VI. POSSIBLE P_4 TERM

The angular distribution at the lowest temperatures show no evidence for a possible contribution from the term $a_4G_4(T)P_4(\cos\theta)$.

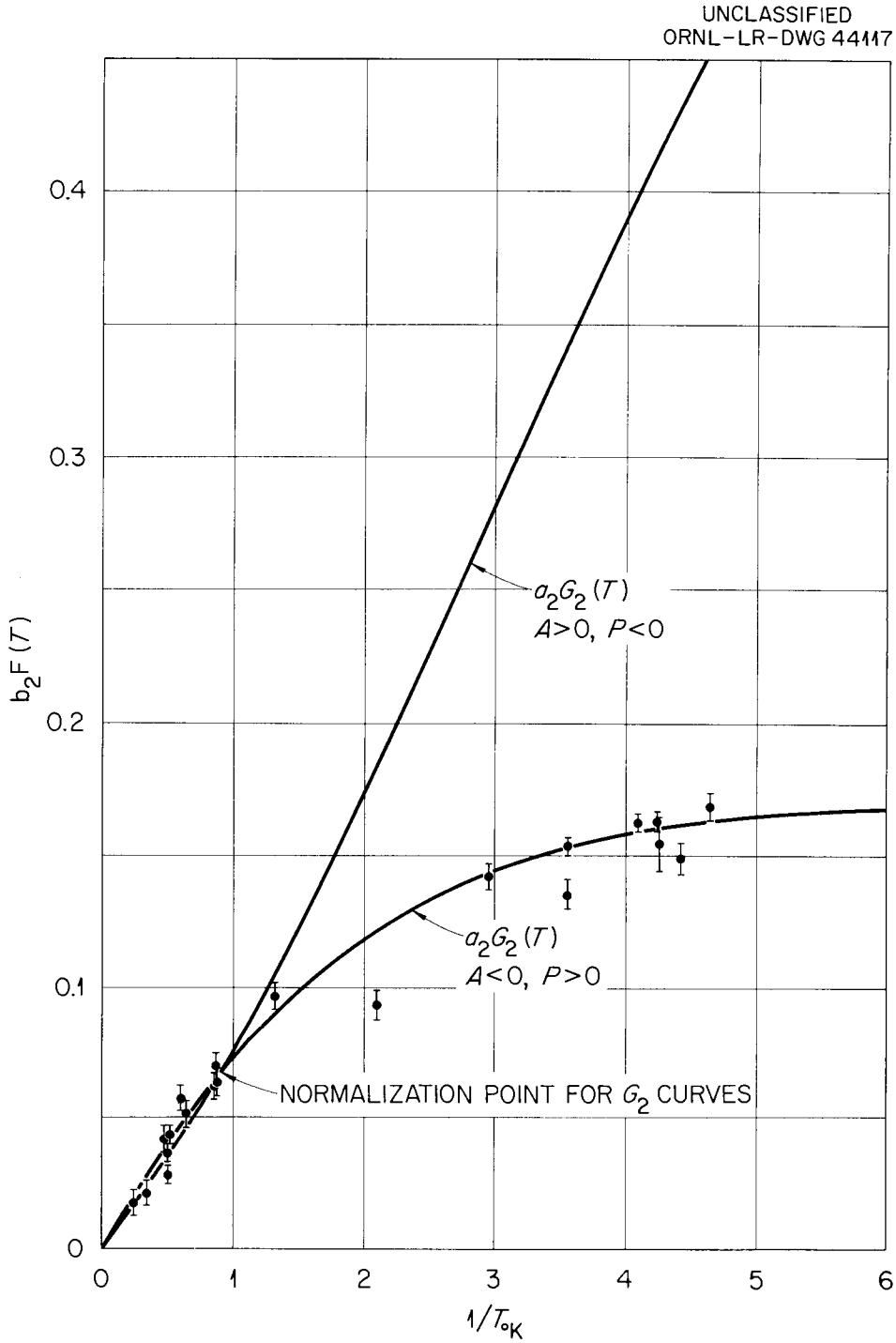

Figure 22. Size of anisotropy as a function of temperature, compared with the normalized theoretical curves of $a_2G_2(T)$ for the two possible sign choices for A and P.

CHAPTER VI

DISCUSSION OF RESULTS

In Figure 22, the experimentally determined alpha-particle anisotropy [coefficient of $P_2(\cos\theta)$] is plotted as a function of sample temperature, over the temperature range 0.2 - 4.2°K. Also shown in Figure 22 are two curves of the anisotropy predicted from the experimentally determined spin Hamiltonian, for the two possible sign choices. It is evident that the data are in satisfactory agreement with the curve for the sign choice $A < 0$, $P > 0$. The alternative sign choice $A > 0$, $P < 0$, is clearly excluded. Figure 2, page 16, is therefore drawn correctly (rather than inverted).

At the absolute zero of temperature, all of the nuclei would be in the state given by the first line of Table I, page 15, which is predominately a state for which $m_I = \pm\frac{3}{2}$. At 0.2°K, however, the lowest three substates have substantially equal populations, since their total splitting is only 0.06°K. At this temperature, the states with $m_I = \pm\frac{1}{2}$ contain 40.4 per cent of all nuclei; the states with $m_I = \pm\frac{3}{2}$ and $\pm\frac{5}{2}$ contain 35.9 per cent and 23.7 per cent respectively. The alignment at 0.2°K is therefore preferentially into the states with $m_I = \pm\frac{1}{2}$, with the angular momentum vector directed approximately perpendicular to the crystalline c axis. The observed enhancement of alpha emission in this direction leads to the conclusion that <u>the alpha-particles are emitted preferentially in the direction of the nuclear angular momentum vector</u>.

This result follows directly from two experimental determinations--the microwave resonance measurements and the present experiment--and holds regardless of any assumptions about nuclear shapes or the mechanism of alpha-particle emission. Under the usual assumption for this region of the Periodic Table that the nuclear angular momentum vector is oriented along the nuclear symmetry axis,[59] the experimental result means that the alpha particles are emitted preferentially along the nuclear symmetry axis.

The electric quadrupole moment of the neptunium-237 nucleus has not been measured. In the neighboring nuclides uranium-233 and -235, optical hyperfine spectra have been interpreted[60-62] as giving evidence for $Q > 0$ in both cases. Considerations based on nuclear systematics predict a positive quadrupole moment for these uranium isotopes and for neptunium-237. In a recent summary[63] of energy-level assignments in the region $A > 225$, Stephens, Asaro, and Perlman have correlated known data with the level diagrams which were calculated by Nilsson[64] for nuclei

---

[59] F. Villars, Annual Review of Nuclear Science 7, 223 (1957).

[60] Vander Sluis and McNally, loc. cit., and also private communication.

[61] A. G. Zimin and N. M. Iashin, Soviet Phys.--Doklady 1, 419 (1956).

[62] N. I. Kaliteevskii and M. P. Chaika, Optika i Spektroskopiya 1, 809 (1956).

[63] F. S. Stephens, F. Asaro, and I. Perlman, Phys. Rev. 113, 212 (1959).

[64] S. G. Nilsson, Kgl. Danske Videnskab. Selskab, Mat.-fys. Medd. 29, No. 16 (1955).

with large deformations. Stephens, et al., conclude that the model is generally reliable, and that "in no case were accurate data available that indicated an assignment significantly at variance with the expectations of the theory."[65] This theory and its agreement with experimental data have also been reviewed recently by Mottelson and Nilsson.[66] The theory predicts that all nuclei in this region are prolate, and its wide range of agreement with experimental data may be taken as support for $Q > 0$ for uranium-233 and -235, as well as for neptunium-237. If the quadrupole moment of neptunium-237 is indeed positive, then the experiment has shown that the alpha particles are emitted preferentially from the "tips" of the prolate nucleus, in agreement with the barrier penetration picture.[67] However, this is inconsistent with the "column-of-charge" model[68] of the electronic structure of the neptunyl ion, which predicts that P and Q are of opposite sign.

In a recent publication, Pryce[69] has suggested that neptunium-237 has a negative quadrupole moment. This would reconcile the experimentally determined sign of P with the "column-of-charge" picture. In this case, however, the experimental result would have to be interpreted as showing alpha-particle emission preferentially from the "flat" sides of the

---

[65] Stephens, Asaro, and Perlman, op, cit., p. 214.

[66] Mottelson and Nilsson, loc. cit.

[67] Hill and Wheeler, loc. cit.

[68] Eisenstein and Pryce, loc. cit.

[69] Pryce, loc. cit.

oblate nucleus, contrary to the predictions of the barrier penetration theory. It can thus be seen that the experimental results on the sign of P and the direction of preferential alpha-particle emission place the two theories in direct conflict. If barrier penetration is the controlling factor in alpha emission, then the electronic configuration in the neptunyl ion cannot be the simple "column of charge" given by Eisenstein and Pryce. On the other hand, if the chemical and electronic arguments are correct, then barrier penetration cannot play the determining role in alpha emission.

When uranium-233 and -235 nuclei were aligned by cooling a sample of uranyl rubidium nitrate, the alpha particles from these nuclei were also emitted preferentially perpendicular to the crystalline c axis.[70, 71] The hyperfine coupling in the uranyl salt has not been measured, but it is presumably of purely quadrupolar character [A = 0 in Equation (1)], since the uranyl ion is essentially nonmagnetic.[72] The "column-of-charge" model would also predict that P is opposite in sign to Q in the uranyl ion, so the experimental results on the two uranium isotopes also place the two theories in conflict.

---

[70] Roberts, Dabbs, and Parker, loc. cit.

[71] J. W. T. Dabbs, L. D. Roberts, and G. W. Parker, Physica XXIV, S.69 (1958).

[72] Eisenstein and Pryce, loc. cit.

BIBLIOGRAPHY

Berman, R. "Some Experiments on Thermal Contact at Low Temperatures," Journal of Applied Physics 27 (1956) 318-23.

Bethe, H. A. and J. Ashkin. "Passage of Radiations Through Matter," in E. Segre (ed.). Experimental Nuclear Physics, Vol. 1. New York: John Wiley and Sons, Inc., 1953.

Bleaney, B., P. M. Llewellyn, M. H. L. Pryce, and G. R. Hall. "Paramagnetic Resonance in Neptunyl Rubidium Nitrate," Philosophical Magazine and Journal of Science 45 (1954) 992-93.

Brattain, W. H. and G. L. Pearson. "Changes in Conductivity of Germanium Induced by Alpha-Particle Bombardment," The Physical Review 80 (1950) 846-50.

Casimir, H. B. G. Magnetism and Very Low Temperatures. Cambridge: University Press, 1940.

Christy, R. F. "Alpha Decay of Spheroidal Nuclei," Bulletin of the American Physical Society 30 (1955) No. 1, 66.

Clement, J. R., J. K. Logan, and J. Gaffney. "Liquid Helium Vapor Pressure Equation," The Physical Review 100 (1955) 743-44.

Clement, J. R. and E. H. Quinnell. "The Low Temperature Characteristics of Carbon-Composition Resistance Thermometers," The Review of Scientific Instruments 23 (1952) 213-16.

Cooke, A. H., H. Meyer, and W. P. Wolf. "A New Method of Correlating the Magnetic Temperature Scales of Paramagnetic Salts Below $1^{o}K$," Proceedings of the Royal Society of London A233 (1956) 536-55.

Dabbs, J. W. T., L. D. Roberts, and G. W. Parker. "Alpha-Particle and Fission Anisotropies from Oriented Actinide Nuclei," Physica XXIV (1958) S.69-S.77.

Dabbs, J. W. T., L. D. Roberts, and G. W. Parker. "Magnetic Susceptibility of $NpO_2Rb(NO_3)_3$ at Liquid Helium Temperatures," Bulletin of the American Physical Society II 2 (1957) 185.

DeBoer, J. "Transport Properties of Gaseous Helium at Low Temperatures," in C. J. Gorter (ed.). Progress in Low Temperature Physics, Vol. I. Amsterdam: North-Holland Publishing Company, 1955.

DeKlerk, D. and M. J. Steenland. "Adiabatic Demagnetization," in C. J. Gorter (ed.). Progress in Low Temperature Physics, Vol. I. Amsterdam: North-Holland Publishing Company, 1955.

Dieke, G. H. and A. B. F. Duncan. Spectroscopic Properties of Uranium Compounds. New York: McGraw-Hill Book Company, Inc., 1949.

Eisenstein, J. C. and M. H. L. Pryce. "The Electronic Structure and Magnetic Properties of Uranyl-like Ions: I. Uranyl and Neptunyl," Proceedings of the Royal Society of London A229 (1955) 20-38.

Francis, J. E., Jr., P. R. Bell, and J. C. Gundlach. "Single-Channel Analyzer," The Review of Scientific Instruments 22 (1951) 133-37.

Gorter, C. J. (ed.). Progress in Low Temperature Physics. Amsterdam: North-Holland Publishing Company, 1955.

Hammel, E. F. "The Low Temperature Properties of Helium Three," in C. J. Gorter (ed.). Progress in Low Temperature Physics, Vol. I. Amsterdam: North-Holland Publishing Company, 1955.

Hill, D. L. and J. A. Wheeler. "Nuclear Constitution and the Interpretation of Fission Phenomena," The Physical Review 89 (1953) 1102-45.

Hoard, J. L. and J. D. Stroupe. Atomic Energy Project Report A-1229, 1943, cited in G. H. Dieke and A. B. F. Duncan. Spectroscopic Properties of Uranium Compounds. New York: McGraw-Hill Book Company, Inc., 1949.

Hodgman, Charles D. (ed.). Handbook of Chemistry and Physics. 40th Ed. Cleveland, Ohio: Chemical Rubber Publishing Company, 1958.

Kaliteevskii, N. I. and M. P. Chaika. "The Ratio of the Magnetic Spin and Quadrupole Moments of the Nuclei U^{233} and U^{235}," Optika i Spektroskopiya 1 (1956) 809-11. See Atomic Energy Commission Translation 2890.

Koenig, S. H. and G. R. Gunther-Mohr. "The Low Temperature Electrical Conductivity of n-Type Germanium," The Physics and Chemistry of Solids 2 (1957) 268-83.

Kurti, N. and F. Simon. "Remarks on the 'Curie' Scale of Temperature," Philosophical Magazine and Journal of Science 26 (1938) 849-54.

Llewellyn, P. M. "Some Applications of Paramagnetic Resonance." Unpublished Doctoral Dissertation, St. John's College, England, 1957.

Mellor, J. W. Comprehensive Treatise on Inorganic and Theoretical Chemistry. 16 vols. London: Longmans, Green and Company, 1932 and 1942.

Mottelson, Ben R. and Sven Gösta Nilsson. "The Intrinsic States of

Odd-A Nuclei having Ellipsoidal Equilibrium Shape," Matematisk-fysiske Skrifter udgivet af Det Kongelige Danske Videnskabernes Selskab 1 (1959) No. 8.

Osborn, J. A. "Demagnetizing Factors of the General Ellipsoid," The Physical Review 67 (1945) 351-57.

Present, R. D. Kinetic Theory of Gases. New York: McGraw-Hill Book Company, Inc., 1958.

Pryce, M. H. L. "Sign of g in Magnetic Resonance, and the Sign of the Quadrupole Moment of Np^{237}," Physical Review Letters 3 (1959) 375.

Roberts, L. D., J. W. T. Dabbs, and G. W. Parker. "Alpha-Particle Emission from Oriented Neptunium-237 and Uranium-233 Nuclei," Proceedings of the Second International Conference on the Peaceful Uses of Atomic Energy, Vol. 15. Geneva: United Nations, 1958. Pp. 322-30.

Rose, M. E. Elementary Theory of Angular Momentum. New York: John Wiley and Sons, Inc., 1957.

Rose, M. E. "Geometrical Corrections for Anisotropically Emitting Sources," Oak Ridge National Laboratory Report 2050 (1956).

Segre, E. (ed.). Experimental Nuclear Physics. 3 vols. New York: John Wiley and Sons, Inc., 1953-1959.

Spiers, J. A. "Angular Distribution of Radioactive Disintegration Products," Nature 161 (1948) 807-9.

Stephens, S. F., F. Asaro, and I. Perlman. "Classification of the Energy Levels of Odd-Mass Nuclei in the Heavy-Element Region," The Physical Review 113 (1959) 212-24.

Strominger, D., J. M. Hollander, and G. T. Seaborg. "Table of Isotopes," Reviews of Modern Physics 30 (1958) 585-904.

Vander Sluis, K. L. and J. R. McNally, Jr. "Nuclear Moments of U^{233} and U^{235}," Journal of the Optical Society of America 44 (1954) 87-88.

Villars, F. "The Collective Model of Nuclei," Annual Reviews of Nuclear Science 7 (1957) 185-230.

Walter, F. J., J. W. T. Dabbs, and L. D. Roberts. "Large Area Germanium Counters," Oak Ridge National Laboratory Report 2877 (1960).

Webb, F. J. and J. Wilks. "The Measurement of Lattice Specific Heats at Low Temperatures Using a Heat Switch," Proceedings of the Royal Society of London A230 (1955) 549-59.

Wheatley, J. C., D. F. Griffing, and T. L. Estle. "Thermal Contact and Insulation below 1°K," The Review of Scientific Instruments 27 (1956) 1070-77.

Zachariasen, W. H. "Crystal Chemical Studies of the 5f Series of Elements. XXIII. On the Crystal Chemistry of Uranyl Compounds and of Related Compounds of Transuranic Elements," Acta Crystallographica 7 (1954) 795-99.

Zimin, A. G. and N. M. Iashin. "The Nuclear Quadrupole Moment of U^{233}," Soviet Physics--Doklady 1 (1956) 419-20.

ORNL-2919
UC-37 Instruments
TID-4500 (15th ed.)

INTERNAL DISTRIBUTION

1. C. E. Center
2. Biology Library
3. Health Physics Library
4-5. Central Research Library
6. Reactor Experimental Engineering Library
7-26. Laboratory Records Department
27. Laboratory Records, ORNL R.C.
28. A. M. Weinberg
29. L. B. Emlet (K-25)
30. J. P. Murray (Y-12)
31. J. A. Swartout
32. E. H. Taylor
33. E. D. Shipley
34. A. H. Snell
35. M. L. Nelson
36. W. H. Jordan
37. G. E. Boyd
38. R. A. Charpie
39. S. C. Lind
40. F. L. Culler
41. A. Hollaender
42. W. M. Good
43. M. T. Kelley
44. J. L. Fowler
45. R. S. Livingston
46. K. Z. Morgan
47. P. M. Reyling
48. T. A. Lincoln
49. A. S. Householder
50. C. P. Keim
51. C. S. Harrill
52. C. E. Winters
53. D. S. Billington
54. H. E. Seagren
55. D. Phillips
56. E. O. Wollan
57. A. J. Miller
58. J. A. Lane
59. R. B. Briggs
60-84. L. D. Roberts
85. R. N. Lyon
86. W. C. Koehler
87. E. P. Blizard
88. M. E. Rose
89. M. J. Skinner
90. J. E. Sherwood
91. R. B. Murray
92. J. A. Harvey
93. A. Simon
94. J. J. Pinajian
95. F. C. Maienschein
96. R. S. Cockreham
97. R. K. Abele
98. H. E. Banta
99. R. L. Becker
100. A. Chetham-Strode
101. H. O. Cohn
102. T. E. Cole
103-127. J. W. T. Dabbs
128. R. A. Dandl
129. R. H. Dilworth
130. S. J. Ditto
131. E. P. Epler
132. J. H. Gibbons
133. P. M. Griffin
134. J. C. Gundlach
135-184. S. H. Hanauer
185. C. H. Johnson
186. E. R. Mann
187. F. K. McGowan
188. J. R. McNally, Jr.
189. R. L. Macklin
190. W. F. Mruk
191. J. H. Neiler
192. L. C. Oakes
193. G. W. Parker
194. G. R. Satchler
195. H. W. Schmitt
196. H. C. Schweinler

197. P. H. Stelson
198. R. S. Stone
199. G. T. Trammell
200. K. L. Vander Sluis
201. W. C. Waggener
202. C. S. Walker
203-205. F. J. Walter
206. T. A. Welton
207. H. B. Willard
208. M. K. Wilkinson
209. H. W. Wright
210. C. A. Preskitt
211. W. Kofink
212. W. R. Brode (consultant)
213. R. F. Christy (consultant)
214. H. Feshbach (consultant)
215. W. A. Fowler (consultant)
216. M. Goldhaber (consultant)
217. A. E. S. Green (consultant)
218. J. O. Thompson (consultant)
219. T. Lauritsen (consultant)
220. M. S. Livingston (consultant)
221. C. Longmire (consultant)
222. N. F. Ramsey (consultant)
223. A. H. Nielsen (consultant)
224. J. R. Richardson (consultant)
225. J. H. Van Vleck (consultant)
226. J. A. Wheeler (consultant)
227. ORNL - Y-12 Technical Library, Document Reference Section

EXTERNAL DISTRIBUTION

228. Division of Research and Development, AEC, ORO
229-845. Given distribution as shown in TID-4500 (15th ed.) Instruments category (100 copies - OTS)